

We are IntechOpen, the world's leading publisher of Open Access books Built by scientists, for scientists

6,900

Open access books available

186,000

International authors and editors

200M

Downloads

Our authors are among the

154

Countries delivered to

TOP 1%

most cited scientists

12.2%

Contributors from top 500 universities



WEB OF SCIENCE™

Selection of our books indexed in the Book Citation Index
in Web of Science™ Core Collection (BKCI)

Interested in publishing with us?
Contact book.department@intechopen.com

Numbers displayed above are based on latest data collected.
For more information visit www.intechopen.com



Diffuse Emission of ^{26}Al and ^{60}Fe in the Galaxy

Wei Wang

National Astronomical Observatories, Chinese Academy of Sciences, Beijing

China

1. Introduction

The Universe is a huge factory of the elements. Just 3 minutes after the big bang, primordial nucleosynthesis occurred (original idea by Gamow 1946). The big bang nucleosynthesis (BBN) produces the present abundance of light elements: D (Deuterium), ^3He , ^4He , ^7Li . But the heavier elements ($A > 12$) cannot be produced during BBN. Some light elements, e.g. B, Be and ^6Li , are produced by cosmic ray spallation processes. But the heavier elements are mainly produced by nucleosynthesis in stars (see details in a review by Burbidge et al. 1957; Wallerstein et al. 1997).

Cosmic element abundance could be measured precisely by astronomical observations over a wide range of the electromagnetic spectrum, specially in the optical and infrared bands. Anyway, optical, infrared, and ultraviolet observatories provide only a part of the information. Observations of gamma-ray lines from radioactive isotopes open a new window of observations and guide our understanding of nucleosynthesis in stars. Radioactive decays can be studied by measuring γ -ray line spectra of celestial sources. The γ -ray lines can identify the individual isotope, and the abundance of these isotopes can be quantified with the measurement of γ -ray line intensity of the sky. In particular, γ -ray line photons are nearly transparent for the universe, with no absorption by the very dense molecular clouds and interstellar medium. So detections of these γ -ray lines are a powerful tool to study the cosmic abundance of radioactive isotopes.

Two long-lived radioactive isotopes ^{26}Al and ^{60}Fe have the similar half-life (about million years) and astrophysical origins in the Galaxy. Their nucleosynthesis and ejection into the interstellar medium (ISM) are dominated by massive stars and the subsequent core-collapse supernova explosions (Diehl & Timmes, 1998; Prantzos & Diehl, 1996). Detections of these isotopes provide direct evidence that nucleosynthesis is ongoing in the Galaxy. Their line shapes reflect the dynamics of the ejected isotopes in the interstellar medium and then probe properties of ISM and Galactic rotation effect. Measurements of gamma-ray fluxes of ^{26}Al and ^{60}Fe in the Galaxy provide the unique way to constrain the nuclear reaction rates and stellar evolution models.

Cosmic gamma-ray line signals are very weak, and the gamma-ray photons are absorbed by the atmosphere. The detection of Galactic radioactivity must be based on the gamma-ray detectors aboard balloons and spacecrafts. The first gamma-ray line observations were from OSO-3, OSO-7 in 1960's, which revealed the strong 2.223 MeV line from solar flares (Brandt, 1969). This line results from the formation of deuterium via the union of a neutron and proton; in a solar flare the neutrons appear as secondaries from interactions of high-energy

ions accelerated in the flare process. And the field of gamma-ray line astronomy took great leaps forward with the HEAO C, the COS-B (1975-1982) and the Solar Maximum Mission (launched in 1980) satellites. The HEAO C first detected the 1809 keV line from radioactive ^{26}Al in the inner Galaxy (Mahoney et al., 1982). In 1977, NASA announced plans to build a "great observatory" for gamma-ray astronomy. The Compton Gamma-Ray Observatory (CGRO) was designed to take advantage of the major advances in detector technology during the 1980s, and was launched in 1991. The COMPTEL telescope aboard CGRO first mapped the 1809 keV γ -ray line emission of the whole sky (Diehl et al., 1995a; Plüschke et al., 2001), and first detected the strong and broad ^{44}Ti line around 1157 keV from a young supernova remnant (SNR) Cas A (Iyudin et al., 1994). The OSSE telescope aboard CGRO also firstly mapped the 511 keV annihilation line emission in the inner Galaxy (Purcell et al., 1997). Currently, the main space-based gamma ray observatory is the *INTE*rnational Gamma-Ray Astrophysics Laboratory (INTEGRAL). The spectrometer aboard INTEGRAL (SPI) provides the high spectral resolution enough to resolve astrophysical lines and allow spectroscopy in the regime of gamma-rays.

Gamma-ray emissions of ^{26}Al and ^{60}Fe in the Galaxy are studied with the high spectral resolution INTEGRAL spectrometer (SPI). Observations of diffuse ^{26}Al and ^{60}Fe emission and their line shapes in the Galaxy and active nearby star-formation regions with SPI are main scientific objectives in this chapter.

2. Origin of Galactic ^{26}Al and ^{60}Fe

2.1 ^{26}Al

^{26}Al is an unstable nucleus, produced almost exclusively by proton capture on ^{25}Mg in a sufficiently hot environment (Woosley, 1986), mainly destroyed by the β^+ decay into ^{26}Mg since the competing destruction process, i.e., the $^{26}\text{Al}(p, \gamma)^{27}\text{Si}$ reaction, becomes efficient for $T > 5 \times 10^7$ K, and the end of central the H burning barely reaches such a temperature (see the reaction chains shown in Fig. 1). In addition, the ^{26}Al freshly synthesized must be ejected into the interstellar medium before it is destroyed *in situ*. So its synthesis occurs, essentially in three different specific environments: i.e., the core H burning, the C and Ne convective shells, and the explosive Ne burning. For the hydrostatic nucleosynthesis in the core of stars with convective envelopes, the fresh ^{26}Al requires to be convected away from the hot inner burning region sufficiently fast to prevent destruction, and ejected by strong stellar winds. The present theoretical knowledge of ^{26}Al origin in the Galaxy will be presented. Five possible origins of ^{26}Al are discussed separately: core-collapse supernovae; Wolf-Rayet stars; novae; asymptotic giant branch (AGB) stars; and cosmic-ray nuclear reactions in the interstellar medium.

2.1.1 Core-collapse supernovae

Massive stars (e.g. $M > 8M_{\odot}$) end up as core-collapse supernovae (Type II and Type Ib/c events). Thirty years ago, it has been suggested that ^{26}Al is created in core-collapse supernovae (Arnett, 1977; Ramaty & Lingenfelter, 1977). Explosive ^{26}Al nucleosynthesis is triggered by the shock wave in the Ne burning shell (Woosley & Weaver 1980) and ^{26}Al production can be enhanced by neutrino-induced nuclear reactions (Woosley et al., 1990).

Significant ^{26}Al production occurs in both the late pre-supernova phases and explosion processes. In general, the larger the mass, the larger amount of ^{26}Al survives the explosion

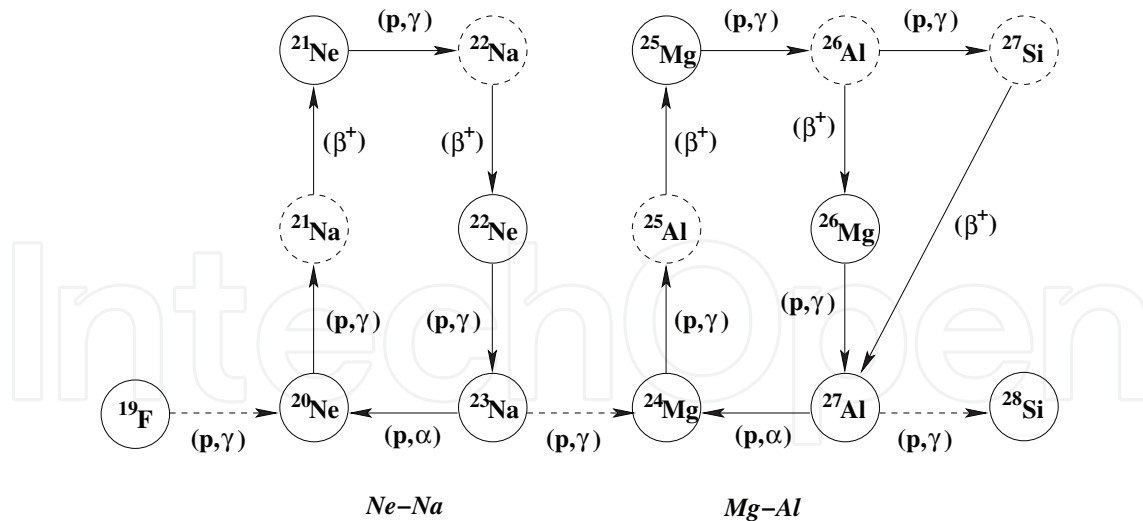


Fig. 1. Reactions of the Ne-Na and Mg-Al chains. Unstable isotopes are denoted by dashed circles (from Rolfs & Rodney 1994).

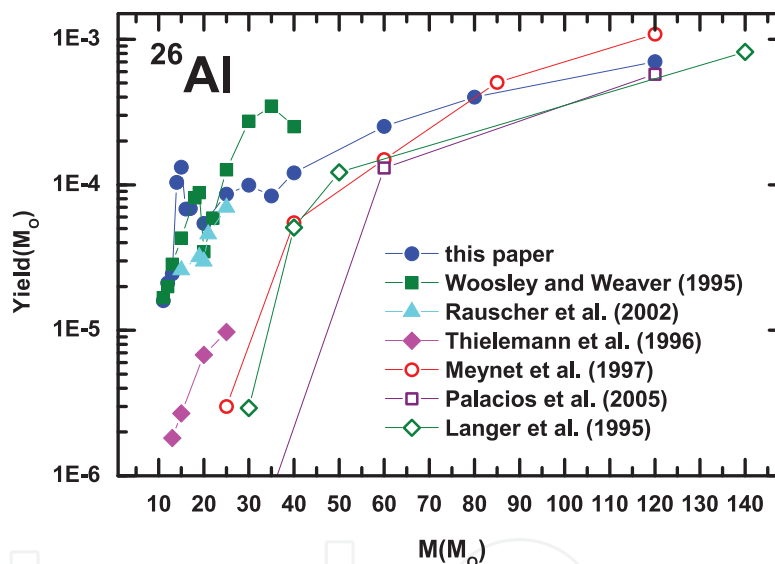


Fig. 2. ^{26}Al yields in different processes (C/Ne convective shells, explosion, winds in the WR star phase) as a function of the initial stellar mass (from recent calculations by Limongi & Chieffi 2006).

(Woosley & Weaver 1995; Rauscher et al. 2002; Limongi & Chieffi 2006). The triangles in Fig. 2 show the ^{26}Al yield produced in C/Ne convective shells that survived to the explosion as a function of the initial mass. The explosive ^{26}Al yield is generally a little higher than pre-supernova production with the different initial masses (Limongi & Chieffi 2006). But different models may have different predictions, e.g., the explosive ^{26}Al is low compared to pre-supernova production for stars with masses higher than $35M_{\odot}$ (Weaver & Woosley, 1993). Typically, the ^{26}Al yields from core-collapse supernovae range from $2 \times 10^{-5} - 5 \times 10^{-4}M_{\odot}$ with initial star masses of $12 - 120M_{\odot}$ (see Fig. 2).

2.1.2 Wolf-Rayet stars

Hydrostatic core H burning in the main sequence stars can produce large amounts of ^{26}Al . At central H exhaustion, the ^{26}Al is located in the He core and in the region of variable H left behind by the receding convective core. Since the He burning easily and quickly destroys the ^{26}Al (via the (n, α) and (n, p) reactions), the amount of ^{26}Al synthesized by central H burning and possibly preserved up to the explosion is just the one located in the H-rich layers plus the one locked in the fraction of the He core that would not be affected by the He burning. If the dredge-up and the mass-loss were not effective, ^{26}Al would mostly decay before it could be ejected by the explosion.

Stars with masses between $10 - 35 M_{\odot}$ will undergo a dredge-up episode that does not enter into the He core, and the mass-loss is weak. Since the He convective shell extends almost up to the base of the H burning shell, only a tiny amount of ^{26}Al which is present in the region of variable H left by the receding H convective core and engulfed in the convective envelope, would be ejected into the interstellar medium. Stars more massive than $35 M_{\odot}$ do not show dredge-up episodes, but the mass-loss is so strong that a substantial fraction of the He core is ejected through stellar winds, i.e., the Wolf-Rayet phase (van der Hucht et al., 1988). For the Wolf-Rayet stars, a large amount of ^{26}Al present in the He core is thus preserved from the destruction and ejected into the interstellar medium. So the main ^{26}Al production in the ISM before supernova explosions comes from the stellar winds of Wolf-Rayet stars. The average yield of ^{26}Al production during the Wolf-Rayet phase ranges from $1 \times 10^{-5} - 3 \times 10^{-4} M_{\odot}$ for with initial star masses of $35 - 120 M_{\odot}$ (Limongi & Chieffi, 2006; Palacios et al., 2005).

From the all-sky survey of 1809 keV emission by COMPTEL (Plüschke et al. 2001), the ^{26}Al in the interstellar medium is predominantly synthesized in massive stars, through the strong stellar winds of Wolf-Rayet stars and core-collapse supernova explosions. The total ^{26}Al yields due to two processes have been calculated by different work (e.g., Limongi & Chieffi 2006; Woosley & Weaver 1995; Langer et al. 1995; Meynet et al. 1997; Thielemann et al. 1996; Rauscher et al. 2002; Palacios et al. 2005). The average ^{26}Al yields provided by various work range from $(0.3 - 30) \times 10^{-5} M_{\odot}$ for $10 - 35 M_{\odot}$ stars, and from $(1 - 10) \times 10^{-4} M_{\odot}$ for stars above $35 M_{\odot}$ (also see Fig. 2). The calculations of the total ^{26}Al yield would be directly compared with the observational limits. Knödlseder (1999) argued that most of ^{26}Al in the Galaxy comes from WR stars, and the study of ^{26}Al in the Cygnus region is a way to resolve this argument.

2.1.3 Novae

^{26}Al production requires moderate peak temperatures, e.g., $T_{\text{peak}} < 2 \times 10^8$ K, and a fast decline from maximum temperature (Ward & Fowler, 1980). These conditions are commonly achieved in nova outbursts. In 1980s, one-zone model calculations of explosive H-burning nucleosynthesis with solar or CNO-enhanced envelopes (Hillebrandt & Thielemann, 1982; Wiescher et al., 1986) suggested that classical novae might produce sufficient amounts of ^{26}Al to account for some of the observed meteoritic anomalies but would not represent major Galactic sources. New calculations on the basis of ONeMg white dwarf stars (Nofar et al., 1991; Weiss & Truran, 1990) produced large amounts of long-lived radioactive nuclei, such as ^{22}Na and ^{26}Al , concluding that the ONe novae might be important sources of the Galactic ^{26}Al . Furthermore, the production of ^{26}Al by novae is very sensitive to the initial composition

of the envelope and to the nuclear reaction rates adopted. ONe novae should be more important ^{26}Al sources than CO novae, because seed nuclei for the Ne-Na and Mg-Al cycles are almost absent in CO novae. For the same reason, the amount of ^{26}Al synthesized in ONe novae depends on the initial composition of the white dwarf core. Some improvements in the nuclear reaction rates since Caughlan & Fowler (1988) would lead to a lower ^{26}Al production. Recent hydrodynamic calculations of nova outbursts (Jose et al., 1997) predict that the ejected ^{26}Al mass by ONe novae ranges from $(0.3 - 1.7) \times 10^{-8} M_{\odot}$ considering various white dwarf masses and accretion rates.

The amount of ^{26}Al ejected into the interstellar medium by ONe novae decreases as the mass of the underlying white dwarf increases (Jose et al., 1997). So the low-mass white dwarfs are most likely candidates for ^{26}Al production, with the higher ^{26}Al production and higher ejected mass. But white dwarfs lower than $\sim 1.1M_{\odot}$ are expected to be CO white dwarf, which are unable to produce important quantities of ^{26}Al . Then the maximum ejection mass of ^{26}Al by one ONe nova event would be $\sim 2 \times 10^{-8}M_{\odot}$. The predicted contribution of nova outbursts to the Galactic ^{26}Al ranges $(0.1 - 0.4) M_{\odot}$, which is small compared with the present observational limits ($M_{\text{gal}}(^{26}\text{Al}) \sim 2 M_{\odot}$) derived by COMPTEL measurements (Diehl et al., 1995a) and INTEGRAL/SPI (Diehl et al., 2006a; Wang et al., 2009). Hence, novae represent important ^{26}Al sources in the Galaxy, but cannot be the dominant ones, which is consistent with the accepted hypothesis of young populations as major sources of the Galactic ^{26}Al .

2.1.4 Asymptotic giant branch (AGB) stars

The intermediate-mass stars ($1.5 \leq M/M_{\odot} \leq 6$) can evolve through a thermally-pulsing phase with the strong stellar wind, so-called asymptotic giant branch (AGB) stars. AGB stars are characterized by two burning shells, one of helium, and one of hydrogen, and by a deep convective envelope extending from above the H-burning shell up to the surface. ^{26}Al could be produced in three sites of AGB stars: the H-burning shell via Mg-Al chain; the He-burning shell via α -capture on ^{22}Ne , and at the base of the convective envelope in the most massive AGB stars that experience H-burning. In AGB stars, ^{26}Al is efficiently produced by H-burning, but destruction by n-capture reaction during the interpulse and pulse phases becomes increasingly more efficient (Mowlavi & Meynet, 2000).

The ejected ^{26}Al masses by AGB stars depend on the temperature which directly relates to the initial mass, and initial composition. Recent calculations show that the low mass AGB stars ($< 4M_{\odot}$) cannot significantly contribute to ^{26}Al production (Karakas & Lattanzio, 2003; Mowlavi & Meynet, 2000). The AGB star with masses of $4 - 6M_{\odot}$ can yield ^{26}Al in the regime of $(0.2 - 8) \times 10^{-8} M_{\odot}$ (Karakas & Lattanzio 2003). The AGB stars with lower metallicity produce a higher amount of ^{26}Al . The rough estimation of the contribution by AGB stars to the Galactic ^{26}Al varies from $0.01 - 0.4 M_{\odot}$ (Mowlavi & Meynet, 2000). Though the large uncertainties exist for the prediction of ^{26}Al by AGB stars, AGB stars cannot be the main ^{26}Al sources in the Galaxy. But the AGB stars could be best candidates to explain the inferred $^{26}\text{Al}/^{27}\text{Al}$ ratios ranging from $\sim 10^{-4} - 10^{-2}$ observed in meteoritic grains (Clayton & Leising, 1987). As an interesting science, models predict a higher amount of ^{26}Al ($\sim (1 - 2) \times 10^{-7} M_{\odot}$, Mowlavi & Meynet, 2000) around planetary nebulae, which could be possible candidates for direct ^{26}Al detection in future.

Ni52 38 ms 0+	Ni53 45 ms (72-)	Ni54 0+	Ni55 212.1 ms 72-	Ni56 6.077 d 0+	Ni57 35.60 h 32-	Ni58 0+	Ni59 7.6E+4 y 32-	Ni60 0+	Ni61 32-	Ni62 0+	Ni63 109.1 y 12-	Ni64 0+	Ni65 2.5172 h 52-	Ni66 54.6 h 0+	Ni67 21 s (12-)	Ni68 0+
EC β	EC β	EC	EC	EC	EC	68.977	EC	26.223	1.140	3.634	β	0.926	β	β	β	β
Co51	Co52 18 ms	Co53 240 ms (72-)	Co54 193.32 ms 0+	Co55 17.53 h 72-	Co56 72.27 d 4+	Co57 271.79 d 72-	Co58 79.92 d 3+	Co59	Co60 5.2714 y 5+	Co61 1.659 h 72-	Co62 3.59 m 2+	Co63 37.4 s (72-)	Co64 6.39 s 1+	Co65 1.20 s (72-)	Co66 0.23 s (3+)	Co67 0.42 s (72-)
Fe50 150 ms 0+	Fe51 305 ms (52-)	Fe52 8.275 h 0+	Fe53 8.51 m 72-	Fe54 0+	Fe55 2.73 y 32-	Fe56 0+	Fe57 12-	Fe58 0+	Fe59 44.503 d 32-	Fe60 1.5E+6 y 0+	Fe61 5.98 m 32-;52-	Fe62 68 s 0+	Fe63 6.1 s (52-)	Fe64 2.0 s 0+	Fe65 0.4 s 0+	Fe66 0+
EC β	EC	EC	EC	EC	EC	91.72	2.2	0.28	β	β	β	β	β	β	β	β
Mn49 382 ms 52-	Mn50 283.88 ms 0+	Mn51 46.2 m 52-	Mn52 8.51 m 6+	Mn53 3.74E+6 y 72-	Mn54 312.3 d 3+	Mn55 52-	Mn56 2.5785 h 3+	Mn57 85.4 s 52-	Mn58 3.0 s 0+	Mn59 4.6 s 32-;52-	Mn60 51 s 0+	Mn61 0.71 s (52-)	Mn62 0.83 s (3+)	Mn63 0.25 s 0+	Mn64	Mn65
EC	EC	EC	EC	EC	EC	100	EC	100	β	β	β	β	β	β	β	β
Cr48 21.56 h 0+	Cr49 42.3 m 52-	Cr50 1.8E+17 y 0+	Cr51 27.702 d 72-	Cr52 0+	Cr53 32-	Cr54 0+	Cr55 3.497 m 32-	Cr56 5.94 m 0+	Cr57 21.1 s 32-;52-;72-	Cr58 7.0 s 0+	Cr59 0.74 s 0+	Cr60 0.57 s 0+	Cr61	Cr62 0+	Cr63	Cr64
EC	EC	EC	EC	EC	EC	83.789	9.501	2.365	β	β	β	β	β	β	β	β
V47 32.6 m 32-	V48 15.9735 d 4+	V49 330 d 72-	V50 1.4E+17 y 6+	V51 72-	V52 3.743 m 3+	V53 1.61 m 72-	V54 49.8 s 3+	V55 6.54 s (72-)	V56	V57	V58	V59	V60	V61	V62	V63

Fig. 3. The caption of ^{60}Fe produced by neutron capture processes of iron isotopes e.g., ^{56}Fe , and ^{59}Fe β -decay will generate a leak in the ^{60}Fe production.

2.1.5 Cosmic-ray nuclear reactions in the interstellar medium

The interactions of accelerated particles with ambient matter can produce a variety of gamma-ray lines following the de-excitation of excited nuclei in both the ambient matter and the accelerated particles. Nuclear reaction of low energy heavy cosmic-ray particles have been proposed as another ^{26}Al source process (Clayton, 1994). Based on the COMPTEL measurement of excited ^{12}C in the Orion molecular cloud complex (Bloemen et al., 1994), Clayton (1994) suggested that this could be an efficient ^{26}Al source process. The cross sections for the $^{26}\text{Mg}(\text{H},n)^{26}\text{Al}$ and $^{28}\text{Si}(\text{H},ppn)^{26}\text{Al}$ reactions are of the similar magnitude as the one for the $^{12}\text{C}(\text{H},p)^{12}\text{C}$ reaction. Therefore, the estimation for the Orion region of active star formation corresponds to an ^{26}Al yield of $\sim 10^{-4} M_{\odot}$.

The Galactic ^{26}Al yield is quite uncertain, depending on the fractions of molecular clouds irradiated by low-energy cosmic rays. And the absence of substantial Galactic plane 4.4 MeV emission due to ^{12}C de-excitation suggests that this process is probably negligible as a Galactic ^{26}Al source (Ramaty, 1996).

2.2 ^{60}Fe

The radioactive isotope ^{60}Fe is believed to be synthesized through successive neutron captures on Fe isotopes (e.g., ^{56}Fe , see Fig. 3) in a neutron-rich environment inside He shells in AGB stars (^{60}Fe is stored in white dwarfs and cannot be ejected), and massive stars, before or during their final evolution to core collapse supernovae. ^{60}Fe can be also synthesized in Type Ia SNe (Woosley, 1997). It is destroyed by the $^{60}\text{Fe}(n,\gamma)$ process. Since its closest parent, ^{59}Fe is unstable, the $^{59}\text{Fe}(n,\gamma)$ process must compete with the $^{59}\text{Fe}(\gamma^-)$ decay to produce an appreciate amount of ^{60}Fe .

2.2.1 Massive stars

A neutron-rich environment in massive stars is required to produce ^{60}Fe . And a temperature of the order of 2 billion degrees represents an upper limit for the synthesis of ^{60}Fe because above this temperature the (γ,n) and the (γ,p) photon disintegrations of both ^{59}Fe and ^{60}Fe become tremendously efficient. Such an occurrence limits a possible ^{60}Fe production to the He, C, Ne shell burning phases.

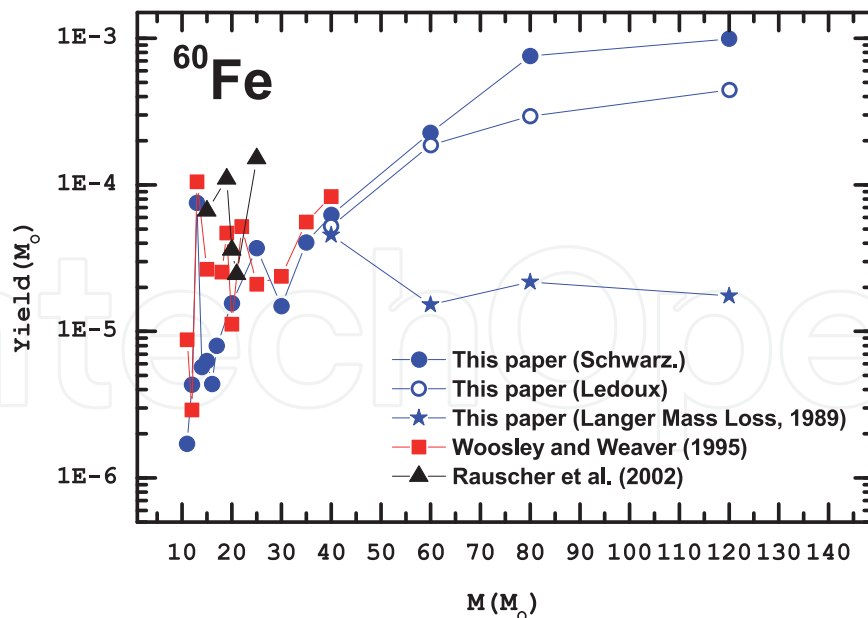


Fig. 4. Comparison among the ^{60}Fe yields as a function of the initial stellar mass provided by various work (from Limongi & Chieffi 2006). The solid and open circles refer to the amount of ejected ^{60}Fe for two different choices of the stability criterion in the He convective shell, i.e., the Schwarzschild and the Ledoux criteria, respectively. The stars represent the amount of ejected ^{60}Fe obtained by adopting the Langer (1989) mass-loss rate for massive stars (WR stars of masses from 40 - 120 M_{\odot}). Solid squares and triangles are the results from Woosley & Weaver (1995) and Rauscher et al. (2002) in the initial mass range of 12 - 40 M_{\odot} .

In He shell burning phases, significant ^{60}Fe production occurs when the star becomes a WR star which experiences such strong mass loss that it first loses all H-rich envelope and then continues eroding the He core up to the moment of the core collapse. In these stars, the He convective shell forms within the region of variable He abundance, then a problem arises of whether the Schwarzschild criterion or the Ledoux one is used to determine if a convective region forms. In Fig. 4, The solid and open circles refer to the amount of ejected ^{60}Fe for two different choices of the stability criterion in the He convective shell. In C shell burning, the high temperature ($> 10^9$ K) allows a large production of α -particles which translates into a high neutron density and hence a large yield of ^{60}Fe . C convective shell could produce a conspicuous amount of ^{60}Fe in stars of the initial mass below 40 M_{\odot} . Ne burning may produce ^{60}Fe , but the lack of an extended and stable convective shell lasting up to the explosion prevents the build up of a significant amount of ^{60}Fe . The average yield of ejected ^{60}Fe in convective shells varies from $10^{-6} - 7 \times 10^{-4} M_{\odot}$, increasing with the initial mass from 11 - 120 M_{\odot} (Limongi & Chieffi, 2006). Calculations by Limongi & Chieffi (2006) suggested the dominant yield of ^{60}Fe in massive stars above 40 M_{\odot} comes from the He convective shell burning, which sensitively depends on the mass-loss rate. Models with a strong mass-loss rate (Langer, 1989) would reduce the ^{60}Fe production during the WR phases into a level of $\sim 10^{-5} M_{\odot}$ (see Fig. 4).

2.2.2 Supernovae

The last episode of synthesis of ^{60}Fe occurs when the blast wave crosses the mantle of the star on its way out during the core-collapse supernova explosions. The peak temperature is of the

order of 2.2×10^9 K, and hence roughly in the same region where the explosive synthesis of ^{26}Al occurs. The average yield of ^{60}Fe in explosion varies from $10^{-5} M_{\odot}$ (initial mass region of $11 - 50 M_{\odot}$) to $4 \times 10^{-5} M_{\odot}$ ($50 - 120 M_{\odot}$).

Fig. 4 shows the total amount of ejected ^{60}Fe as a function of the initial stellar masses (from $11 - 120 M_{\odot}$) calculated by Limongi & Chieffi (2006). The results by the previous work (initial masses from $12 - 40 M_{\odot}$, Woosley & Weaver 1995; Rauscher et al. 2002) are also presented for a comparison. In the initial mass range $< 40 M_{\odot}$, the ^{60}Fe yield by Rauscher et al. (2002) are significantly larger than the yields by both Woosley & Weaver (1995) and Limongi & Chieffi (2006). In Fig. 4, the solid and open circles are obtained by adopting the mass-loss rate by Nugis & Lamers (2000); the stars are obtained by taking the rate by Langer (1989). The mass-loss rate proposed by Langer (1989) is much stronger than the Nugis & Lamers (2000) one. With adopting a stronger mass-loss rate, they have significantly reduce the ^{60}Fe production during the WR phases with the initial masses above $40 M_{\odot}$.

In addition, ^{60}Fe could also be produced in substantial amounts by rare subtypes of SN Ia (Woosley, 1997), which would then be point sources of ^{60}Fe gamma-rays. The average yield of ^{60}Fe in SN Ia is $(1 - 5) \times 10^{-3} M_{\odot}$ depending on models. The ^{60}Fe per event is typically 100 times greater in a high-density white dwarf explosion than in a Type II supernova. With an event rate 10^{-4} yr^{-1} , the composite signal here comes from ~ 100 point sources. A single source at 10 kpc that made $0.005 M_{\odot}$ of ^{60}Fe would be visible for several million years at a flux level of $10^{-7} \text{ ph cm}^{-2} \text{ s}^{-1}$. However, this is well beyond the capability of present gamma-ray telescopes.

3. All-sky observations of ^{26}Al by CGRO/COMPTEL

The 1809 keV gamma-ray line from radioactive ^{26}Al with its decay time of 1 million years can be used as the tracer of the recent nucleosynthesis activity in the Galaxy. Ramaty & Lingenfelter (1979) first predicted the 1809 keV γ -ray line flux of $\sim 10^{-4} \text{ ph cm}^{-2} \text{ s}^{-1} \text{ rad}^{-1}$ from the inner Galaxy, combining the solar ^{27}Al abundance with an estimate of the isotope ratio $^{26}\text{Al} / ^{27}\text{Al}$ ($\sim 10^{-5}$) from supernovae.

The 1809 keV γ -ray line emission was first detected with the Ge spectrometer on the HEAO-C spacecraft (Mahoney et al. 1982). This detection was confirmed by the measurement of Galactic transits through the field of view by the NaI spectrometer on the SMM spacecraft (Share et al., 1985). The following balloon-borne experiments measured the intensity of the ^{26}Al emission and derived some information on its angular distribution (see Durouchoux et al. 1993; Prantzos & Diehl 1996; Schoenfelder et al. 1991; von Ballmoos et al. 1987). And the ^{26}Al fluxes derived from these different measurements depend on the assumed Galactic distribution of ^{26}Al line emission. For example, they found $(1.1 - 4.6) \times 10^{-4} \text{ ph cm}^{-2} \text{ s}^{-1}$ for a point source at the Galactic center, and $(3.9 - 5.4) \times 10^{-4} \text{ ph cm}^{-2} \text{ s}^{-1}$ from the inner Galaxy for a flat supernova model. So mapping the 1809 keV γ -ray line emission of the Galaxy can provide insight into the nature of ^{26}Al sources, and precise determination of the ^{26}Al flux.

The COMPTEL imaging telescope aboard the Compton Observatory performed the first survey of ^{26}Al γ -ray line emission in the whole Galaxy. COMPTEL covered the energy range of 1 - 30 MeV, with an energy resolution of 140 keV (FWHM) around 1809 keV and an angular resolution of 3.8° (see Schoenfelder et al. 1993). COMPTEL has the enough sensitivity to study the origin of ^{26}Al .

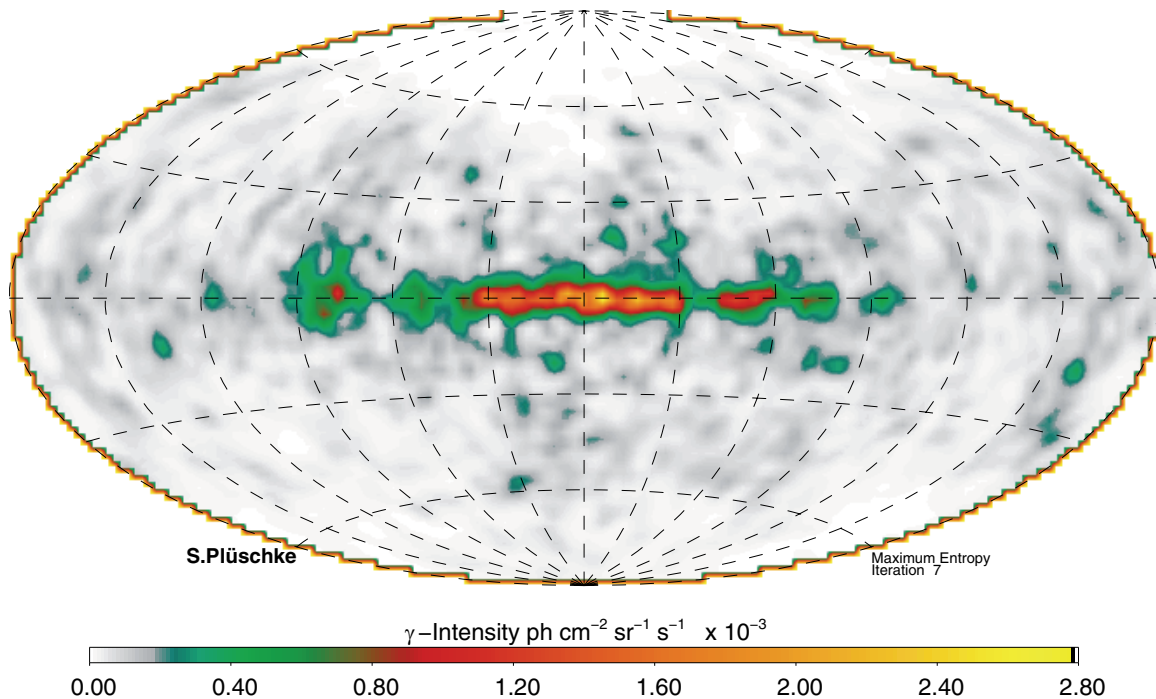


Fig. 5. The maximum-entropy all-sky images of the Galactic 1809 keV line emission observed with COMPTEL over 9 years (from Plüschke et al., 2001).

Diehl et al. (1995a) analyzed the first-year COMPTEL survey data, which has covered the whole Galactic plane. Overlays of the ^{26}Al emission map with the positions of supernova remnants and Wolf-Rayet (WR) stars in the Galaxy suggest that the large-scale structure of ^{26}Al emission in the Galaxy may be contributed to massive stars. And the Vela region (the Vela SNR) shows evidence for a single identified close-by ^{26}Al source (Diehl et al., 1995b). So the first ^{26}Al emission map of the Galactic Plane favors the dominant ^{26}Al origin from massive stars, presumably core-collapse supernovae or Wolf-Rayet stars.

The first 1809 keV all-sky map was presented based on the first three years of COMPTEL observations (Oberlack et al., 1996). The all-sky map confirmed the non-local character of the detected ^{26}Al emission in the first Galactic plane survey (Diehl et al. 1995a). Most of the ^{26}Al emission is attributed to young, massive stars and star-formation regions.

Based on the 9-year COMPTEL observations (1991 – 2000), Plüschke et al. (2001) obtained 1809 keV all-sky map with best significance level. The image (Fig. 5) reconstructions show an extended Galactic ridge emission mostly concentrated towards the Galactic center region ($-30^\circ < l < 30^\circ$), plus an emission feature in the Cygnus region, and a low-intensity ridge along the Carina and Vela regions. These features confirm the previously reported emission structures. In addition, the image shows some low-intensity features in the longitude range between 110° and 270° , e.g. the Orion region (Fig. 5). Near the Galactic center region, the image shows a possible emission from the nearby Sco-Cen region. Also at latitudes beyond $\pm 30^\circ$, some of these low-intensity structures are visible, which may be artifacts, subject to further studies.

In summary, from the all-sky ^{26}Al emission image by COMPTEL, the observed 1809 keV γ -ray line is ascribed to the radioactive decay of ^{26}Al in the interstellar medium. ^{26}Al has been

found to be predominantly synthesized in massive stars and their subsequent core-collapse supernovae. Furthermore, ^{26}Al flux enhancements are detected aligned with regions of recent star formation, such as apparently observed in the Cygnus and Vela regions.

4. INTEGRAL/SPI studies on Galactic ^{26}Al

The INTEGRAL Observatory is an European (ESA) Gamma-Ray Observatory Satellite Mission for the study of cosmic gamma-ray sources in the keV to MeV energy range (Winkler et al., 2003). INTEGRAL was successfully launched from Baikonur Cosmodrome (Kazakhstan) on October 17, 2002 using a Proton rocket provided by the Russian Space Agency. The INTEGRAL orbit is eccentric, with an apogee of 153 000 km, a perigee of 9000 km, and a 3 day period (Jensen et al., 2003). Two main instruments are on board INTEGRAL: the INTEGRAL imager (IBIS) with an angular resolution of $12'$, allowing for source localization with arcmin precise with a field of view of $9^\circ \times 9^\circ$ (Ubertini et al., 2003); the INTEGRAL spectrometer (SPI) with an energy resolution of 2.5 keV at 1.3 MeV and angular resolution of 2.5° within a field of view of $16^\circ \times 16^\circ$ (Vedrenne et al. 2003).

The SPI composed of composed of 19 high purity germanium detectors (GeD) and their associated electronics can allow for high spectral resolution of ~ 2.5 keV at 1 MeV, suitable for astrophysical studies of individual gamma-ray lines and their shapes, e.g. 511 keV line emission, γ -ray lines from radioactivities of ^{26}Al and ^{60}Fe .

^{26}Al is an unstable isotope with a mean lifetime of 1.04 Myr. ^{26}Al first decays into an excited state of ^{26}Mg , which de-excites into the ^{26}Mg ground state by emitting gamma-ray photons with the characteristic energy of 1809 keV (Fig. 6). The study of ^{26}Al line emission from the Galaxy is one of the main science goals of the INTEGRAL mission. SPI aboard INTEGRAL is a high resolution spectrometer with energy resolution of 3 keV (FWHM) at 1809 keV, which therefore adds high-resolution spectroscopic information to ^{26}Al astronomy. The detailed measurement of ^{26}Al line position and shape is expected to reveal more information beyond the COMPTEL imaging survey about the ^{26}Al sources and their location through the Doppler effect, induced from Galactic rotation and dynamics of the ejected ^{26}Al as it propagates in the interstellar medium around its stellar sources.

4.1 Diffuse ^{26}Al emission of the inner Galaxy

The spectral characteristics of ^{26}Al emission in the inner Galaxy serve to study the current nucleosynthesis activity and the properties of the interstellar medium near the ^{26}Al sources on a large-scale averaged scale. We define the “inner Galaxy” as the region $-30^\circ < l < 30^\circ$, $-10^\circ < b < 10^\circ$, and may use this as a representative region for this purpose, since it coincides with the bright ridge of observed 1809 keV emission as observed along the plane of the Galaxy.

Earlier INTEGRAL analysis had used 1.5 years of SPI data to first explore the large-scale spectral characteristics of ^{26}Al emission in the inner Galaxy (Diehl et al. 2006a, 2006b). A detection of the ^{26}Al line from the inner Galaxy with a significance of $\sim 16\sigma$ had confirmed the narrowness of the ^{26}Al line (FWHM < 2.8 keV, 2σ), which had already been seen by RHESSI (Smith et al. 2003) and HEAO-C (Mahoney et al. 1984) earlier.

At present, INTEGRAL/SPI data are accumulated from more than five years to extend this study towards spatially-resolved details of ^{26}Al line spectroscopy across the inner regions of

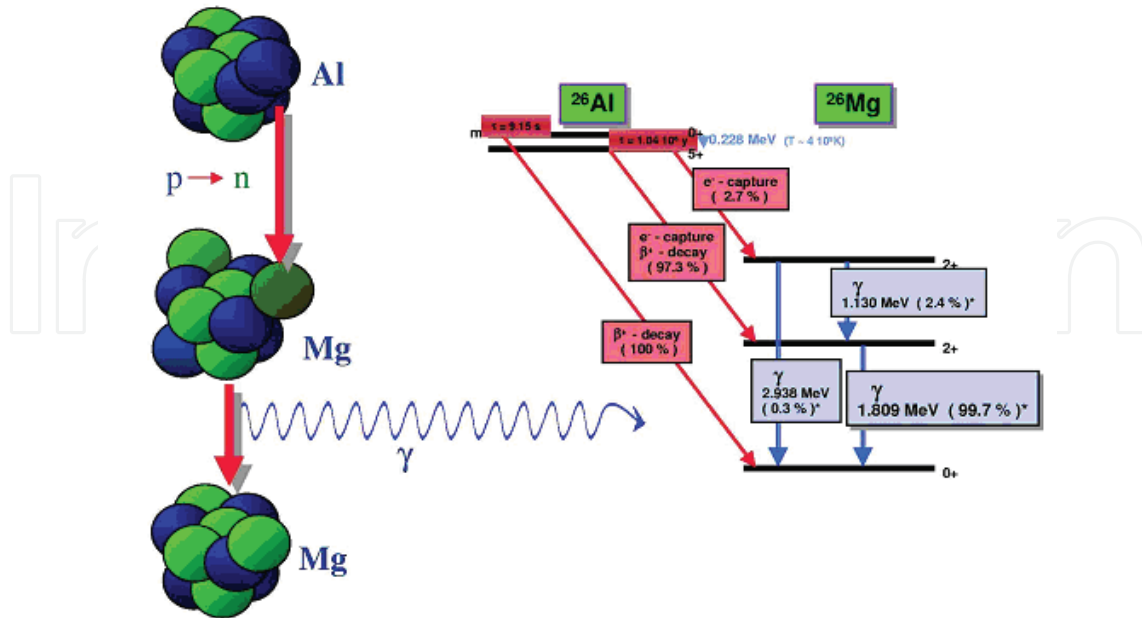


Fig. 6. The decay chain of the radioactive isotope ^{26}Al . ^{26}Al decays with a characteristic lifetime of 1.04 Myr into an excited state of ^{26}Mg , then de-excites into the Mg ground state by emitting γ -ray lines with the energies of 1809 keV (99.7%) and 2.936 keV (0.3%).

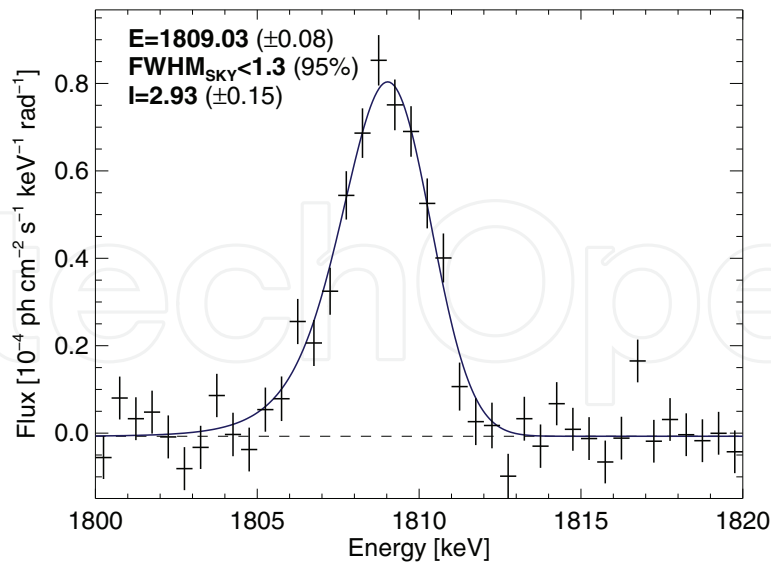


Fig. 7. ^{26}Al spectrum of the inner Galaxy from INTEGRAL/SPI observations (from Wang et al., 2009). The ^{26}Al line width is found to be (< 1.3 keV, 2σ). Fluxes are quoted in units of 10^{-4} ph cm^{-2} s^{-1} rad^{-1} .

the Galaxy. We characterize the ^{26}Al line details through two different approaches. When the sky signal is weak, we fit the spectra with Gaussians plus a linear residual background, and use the Gaussian intensities, centroid energies, and FWHM widths for relative comparisons, such as trends along the plane of the Galaxy. When the signal is sufficiently strong so that we are sensitive to line width details, we describe the line component not by a single Gaussian any more, but rather by the convolution of a Gaussian with the asymmetric instrumental line response. This allows us to infer immediate information about the celestial ^{26}Al dynamics, which we identify with this Gaussian, and in particular its width, which arises from Doppler shifting of the line energies with motion of decaying ^{26}Al nuclei relative to the observer.

Using more than five years of SPI data, the inner-Galaxy ^{26}Al emission spectrum is shown in Fig. 7. The ^{26}Al line is detected at $\sim 28\sigma$ significance. The ^{26}Al gamma-ray flux from the inner Galaxy turns out as $(2.93 \pm 0.15) \times 10^{-4} \text{ ph cm}^{-2} \text{ s}^{-1} \text{ rad}^{-1}$. This is consistent with our earlier values $(3.3 \pm 0.4) \times 10^{-4} \text{ ph cm}^{-2} \text{ s}^{-1} \text{ rad}^{-1}$ (Diehl et al. 2006a, 2006b), and also with the COMPTEL imaging-analysis value of $(2.8 \pm 0.4) \times 10^{-4} \text{ ph cm}^{-2} \text{ s}^{-1} \text{ rad}^{-1}$ (Plüscke et al. 2001). The above value is derived using an asymmetric line shape as best matching our expectations from SPI's spectral response and eventual additional celestial line broadening. The total ^{26}Al gamma-ray flux of the Gaussian fit as determined for the inner Galaxy region is $(2.73 \pm 0.17) \times 10^{-4} \text{ ph cm}^{-2} \text{ s}^{-1} \text{ rad}^{-1}$.

The measured ^{26}Al flux of $(2.93 \pm 0.15) \times 10^{-4} \text{ ph cm}^{-2} \text{ s}^{-1} \text{ rad}^{-1}$ for the inner Galaxy thus translates into a Galactic ^{26}Al mass of $(2.6 \pm 0.6) M_{\odot}$ using a plausible scale height of 180 pc. If we ignored the ejection of ^{26}Al into surrounding cavities and corresponding champagne flows, and used the lower scale heights of O stars or of the molecular disk, we would obtain lower total amounts around or even below $2 M_{\odot}$.

The amount of ^{26}Al is maintained in steady state by a core-collapse supernova rate via $M_{\text{eq}} = \text{SNRate} \cdot \tau \cdot Y$, where the rate is measured in events per year, τ is the mean life of ^{26}Al , and Y is the IMF-averaged ^{26}Al yield in units of M_{\odot} per supernova. The yield in this context must include the explosive yields from the supernova model as well as any ^{26}Al ejected in the Wolf-Rayet wind phase. Yields are moderated by the steep initial mass function (IMF), $\xi \propto m^{-\alpha}$, in our relevant mass range 10–120 M_{\odot} . We use the Miller-Scalo IMF ($\xi \propto m^{-2.7}$) for this higher-mass range (Miller & Scalo, 1979), supported by a wide range of astronomical constraints. Y is obtained from the high-mass initial mass function (IMF) and the nucleosynthesis yields of models. The resulting ^{26}Al yield per massive star is $(1.4 \pm 0.7) \times 10^{-4} M_{\odot}$ based on various published yields as a function of progenitor mass (see Fig. 2). The corresponding supernova rate is $\text{SNRate} = 1.90 \pm 0.95$ events per century (this does not include type Ia supernovae, which have been found to be negligible sources of ^{26}Al). The resulting range of one to three core collapses per century coincides with the recent values obtained from a survey of local O3-B2 dwarfs (Reed, 2005), extrapolated to the Galaxy as whole with spatial distribution models, and the study of the luminosity function of OB associations (McKee & Williams, 1997).

The intrinsic line width is now constrained to $< 1.3 \text{ keV}$ (2σ). In the inner Galaxy, Galactic differential rotation alone can lead to significant Doppler shifts towards specific longitudes where the projected-velocity differences with respect to the solar orbit reach maxima; line broadening results if we integrate over a larger longitude range with different bulk velocity differences. Kretschmer et al. (2003) have simulated the ^{26}Al line shape diagnostics in the inner Galaxy due to Galactic rotation and ^{26}Al ejection from sources, and find that line broadening

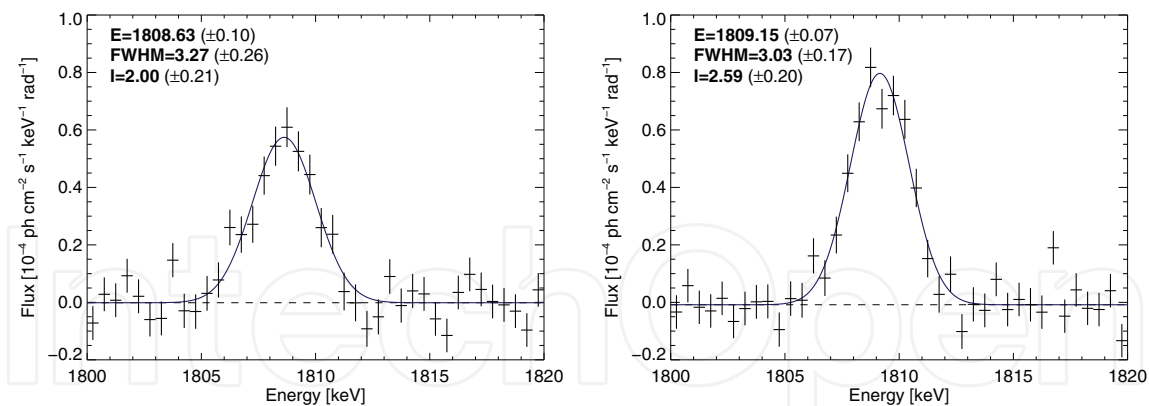


Fig. 8. ^{26}Al spectra for two Galactic quadrants (**left** $0^\circ < l < 60^\circ$, and **right** $-60^\circ < l < 0^\circ$, from Wang et al., 2009). Line centroids relative to the centroid energy of ^{26}Al line in the laboratory (1808.65 keV) show a significant blueshift in the 4th quadrant. Both the spectra have width values near the value of the instrumental line width, implying that ^{26}Al emissions from two quadrants are the narrow lines. In addition, the ^{26}Al flux of the 4th quadrant is higher than that of the 1st quadrant, and the flux ratio is ~ 1.3 .

of up to 1 keV is expected if the signal is integrated over the inner region of the Galaxy. Our present large-scale line-shape constraints are consistent with these expectations. If we interpret line broadening of the ^{26}Al line from the inner Galaxy in terms of interstellar-medium characteristics, the intrinsic-width constraint of < 1.3 keV corresponds to 160 km s^{-1} as a corresponding 2σ limit on ISM velocities. This is well within the plausible and acceptable range for the environment of normal interstellar-medium turbulence (Chen et al. 1997). As a summary, the measured line width of ^{26}Al from the inner Galaxy is consistent with Galactic rotation and modest interstellar-medium turbulence around the sources of ^{26}Al .

4.2 Spectral variations of ^{26}Al gamma-ray line along the Galactic plane

The 9-year COMPTEL imaging of ^{26}Al line emission has already suggested some asymmetry in the inner Galaxy: the fourth Galactic quadrant appears somewhat brighter than the first quadrant (Plüschke (2001) found a significance of 2.5σ for a brightness difference). COMPTEL could provide the image details of ^{26}Al in the Galaxy, but no significant spectral information due to its spectral resolution of about 150 keV near the ^{26}Al line. SPI with its Ge detectors features sufficiently-high spectral resolution to allow astrophysical constraints from ^{26}Al line shapes, averaged over the Galaxy as discussed above, but also for different regions along the Galactic plane due to its imaging properties as a coded-mask telescope.

In this part, we will proceed towards increasing spatial resolution along the Galactic plane, starting out from testing Galactic asymmetries between the first and fourth quadrant. ^{26}Al line parameters toward the different directions of the Galactic plane are determined using separate sky maps covering each sky region, simultaneously fitting these together with our background model to the entire sky survey database. ^{26}Al line fluxes, centroid energies, and line widths then are derived by a simple Gaussian fit to the ^{26}Al line in the resulting spectra, as we are interested in relative changes between different portions of the sky. This will allow us to identify line shifts from bulk motion such as expected from large-scale Galactic rotation,

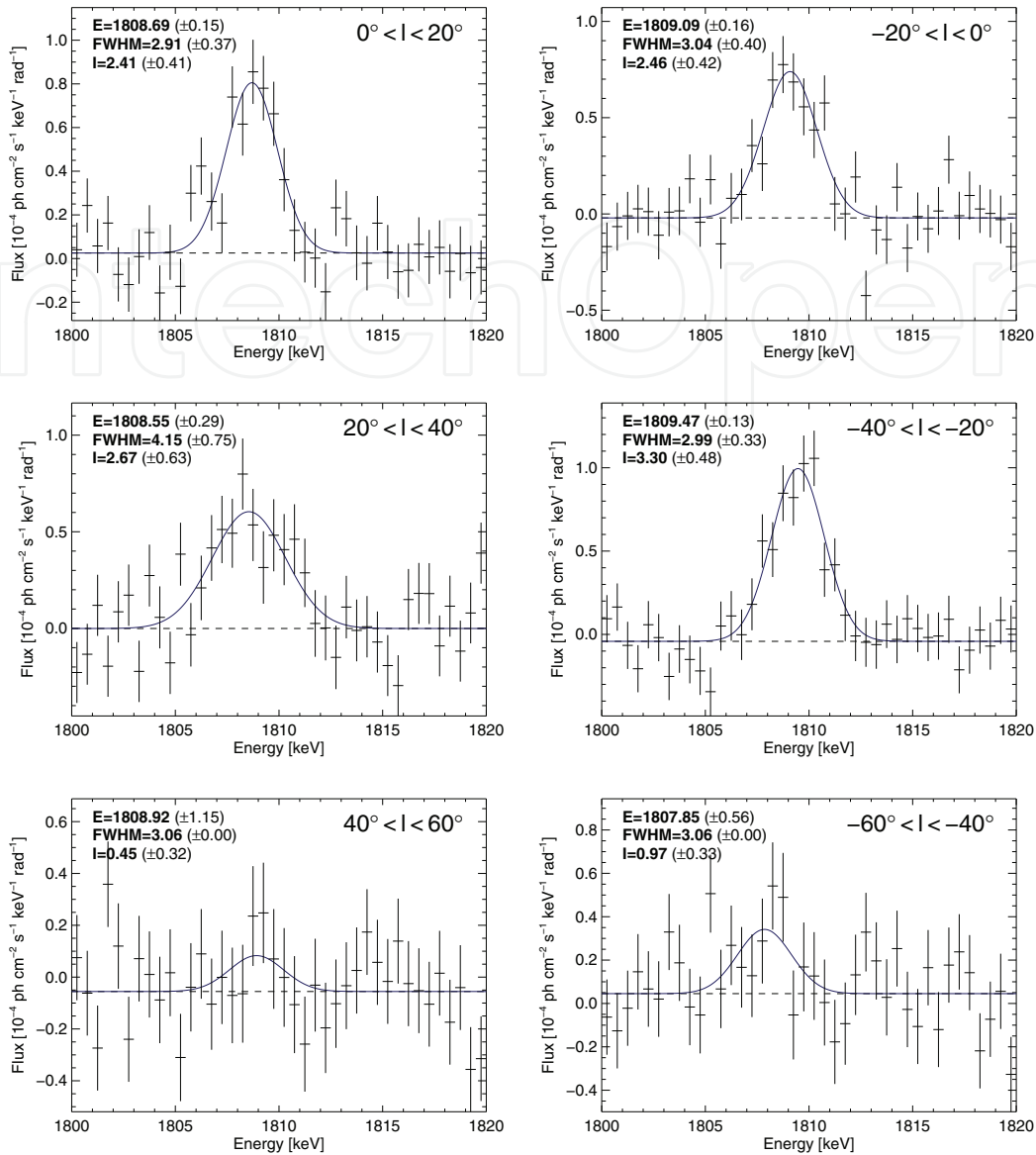


Fig. 9. ^{26}Al spectra of six segments along the Galactic plane ($-60^\circ < l < 60^\circ$, from Wang et al., 2009). Small longitude degree bin (20°) makes the detections of ^{26}Al not significant in the regions of $40^\circ < |l| < 60^\circ$.

and hints for additional line broadenings in particular regions, which would reflect increased ^{26}Al velocities in such regions.

^{26}Al spectra for the 1st ($0^\circ < l < 60^\circ$) and 4th quadrant ($-60^\circ < l < 0^\circ$) are presented in Fig. 8. In the 4th quadrant we note a blueshift of 0.49 ± 0.07 keV relative to the centroid energy of ^{26}Al line in the laboratory, but no significant redshift in the 1st quadrant is apparent ($\sim 0.04 \pm 0.10$ keV). Both spectra have width values compatible with no significant ^{26}Al line broadenings. The indicated ^{26}Al asymmetry between the two inner Galactic quadrants appears again, with a flux ratio of $\sim 1.3 \pm 0.2$.

Challenging the imaging capability of SPI for diffuse and extended emission, we refine spatial structure even more towards smaller longitude intervals. In Fig. 9, we present the spectra

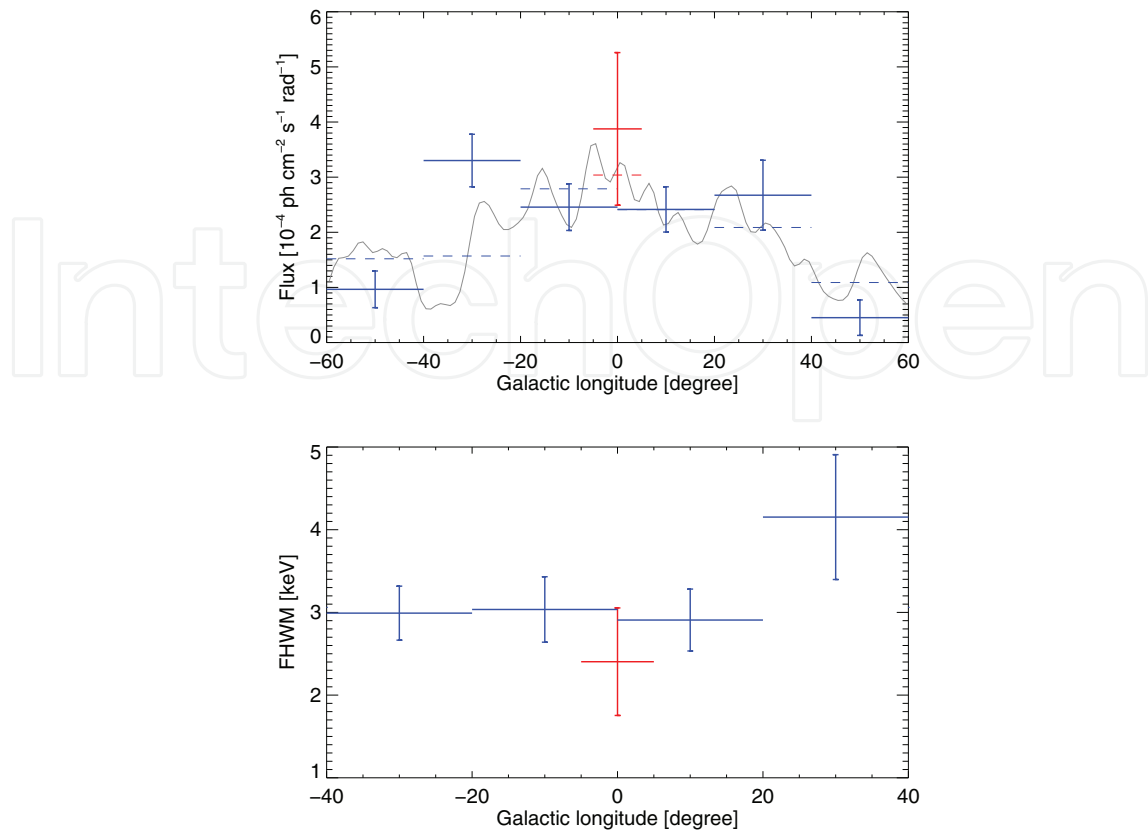


Fig. 10. **Top** ^{26}Al intensity distribution along the Galactic plane (from Wang et al., 2009). For comparison, the COMPTTEL-derived ^{26}Al intensity profile is shown (solid line, and dashed lines when integrated over the same longitude bins). **Bottom** ^{26}Al FWHM (Gaussian fitting) variation along the Galactic longitudes, a broad ^{26}Al line feature is detected toward the longitudes $20^\circ < l < 40^\circ$ (from Wang et al., 2009).

of ^{26}Al emission line for six smaller longitude intervals of 20 degree width along the Galactic plane ($-60^\circ < l < 60^\circ$). The ^{26}Al line is still detected for the inner Galaxy ($-40^\circ < l < 40^\circ$, $> 6\sigma$ for each 20° bin region), but only marginal for the two outer regions ($40^\circ < l < 60^\circ$ and $-60^\circ < l < -40^\circ$, $< 4\sigma$). This may be attributed to both less ^{26}Al brightness and to less exposure in these regions, compared to the inner Galaxy.

Fig. 10 shows the intensity distribution of ^{26}Al emission (from the same 20° regions) along the Galactic plane, adding the (longitude-range normalized) Galactic-Center region ^{26}Al intensity ($|l| < 5^\circ$) for comparison. The variability of ^{26}Al intensity along the Galactic plane again is evident.

We note that the ^{26}Al line in the region of $20^\circ < l < 40^\circ$ appears somewhat broadened, with a Gaussian width of $\text{FWHM} \sim 4.15 \pm 0.75$ keV. This may hint towards a peculiar ^{26}Al source region towards this direction, which could be associated with the Aquila region (Rice et al. 2006). Broadening could result from higher turbulence if the ^{26}Al source region is younger than average and dominated by the ^{26}Al ejection from more massive stars (see Knödlseeder et al. 2004). Further studies would be interesting, and have the potential to identify star formation otherwise occulted by foreground molecular clouds.

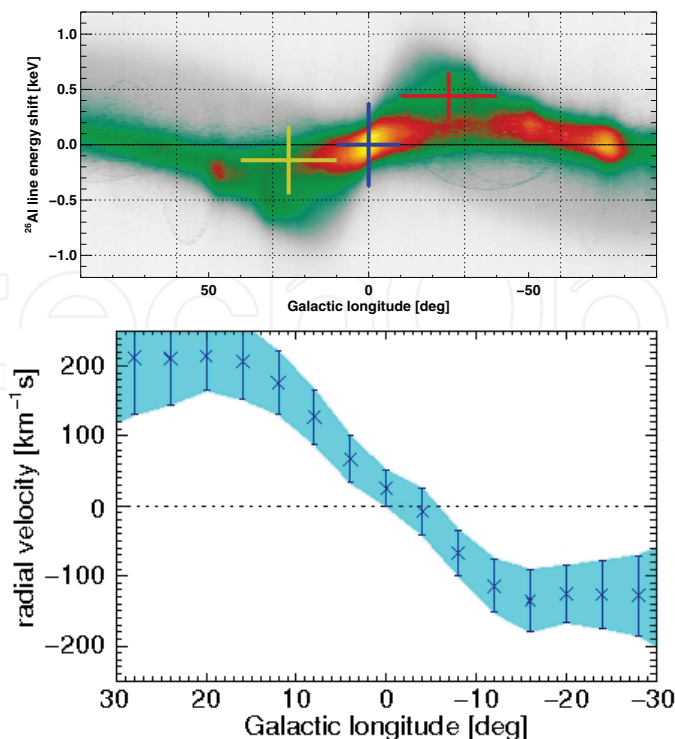


Fig. 11. ^{26}Al line energy shifts along the Galactic plane. Galactic rotation will shift the observed ^{26}Al line energy due to the Doppler effect, to appear blueshifted at negative longitudes and redshifted at positive longitudes. (**Top**) The ^{26}Al line shifts according to the 1.5-year SPI data ($-40^\circ < l < 40^\circ$, $-10^\circ < b < 10^\circ$, Diehl et al. 2006a). Colour scales are expectations of ^{26}Al line positions and intensity modelled from the Galactic rotation curve and a three-dimensional distribution of ^{26}Al sources (Kretschmer et al., 2003). Using the central Galactic region ($-10^\circ < l < 10^\circ$) as a reference (fitted line energy 1808.72 keV), we found centroid energy shifts of -0.14 keV ($10^\circ < l < 40^\circ$) and +0.44 keV ($-40^\circ < l < -10^\circ$), respectively. (**Bottom**) Radial velocity curve of ^{26}Al ejecta in the stellar medium along Galactic longitudes which shows Doppler shifts of the 1809 keV gamma-ray line from ^{26}Al due to Galactic rotation according to more than 6 years of SPI data on the Galactic plane ($-40^\circ < l < 40^\circ$, $-5^\circ < b < 5^\circ$, Kretschmer 2011).

4.3 ^{26}Al line centroid energy as probe of Galactic rotation

Galactic differential rotation can result in not only the broadening of ^{26}Al line but also the shifts of the line centroid energy due to the Doppler effect (Gehrels & Chen, 1996; Kretschmer et al., 2003). Galactic rotation would induce the ^{26}Al line centroid energy redshifts in the 1st quadrant and blueshifts in the 4th quadrant. The Galactic rotation curve can be also determined from observations of various objects (e.g., HI, CO, HII, Brand & Blitz 1993).

The first study on the Doppler shifts of ^{26}Al line due to Galactic rotation using the 1.5-year SPI data was present in Fig. 11 top panel (Diehl et al. 2006a). Using the central Galactic region ($-10^\circ < l < 10^\circ$) as a reference (fitted line energy 1808.72 keV), we found centroid energy shifts of -0.14 keV ($10^\circ < l < 40^\circ$) and +0.44 keV ($-40^\circ < l < -10^\circ$), respectively. Though the error bars for the line positions are very large, we concluded that the results of the line energy shifts are consistent with the Galactic rotation effect (Diehl et al. 2006a).

Recently, using more than 6 years of INTEGRAL/SPI data, Kretschmer (2011) obtained the radial velocity curve of ^{26}Al ejecta along Galactic longitudes with much better resolution (see Fig. 11 bottom panel). The measurements show the characteristic wave-like shape of velocity offset versus Galactic longitude due to the large-scale Galactic rotation. This has been observed for molecular and atomic gas in our and other galaxies. But with ^{26}Al gamma-rays, we get unique access to kinematics of the tenuous, diluted, and presumably hot phase of the interstellar medium, as it is expected around the massive stars which eject radioactive ^{26}Al in the Galaxy. We should note that comparing the velocity curves from ^{26}Al line shape measurements along the Galactic plane and other observations and theory found that the hot gas of ^{26}Al ejecta undergoes additional acceleration in the direction of Galactic rotation.

4.4 Latitudinal variations of ^{26}Al emission

The interpretation of ^{26}Al imaging and spectral results relies on (uncertain) distances of ^{26}Al sources. Along the line-of-sight, the detected ^{26}Al signal could originate from local star-formation complexes (~ 100 pc), or from the nearest part of the Sagittarius-Carina arm (1 – 2 kpc), or from the Galactic center region (~ 8 kpc), or even from the distant side of the Galaxy (> 10 kpc). In this section, we try a possible way to resolve the ^{26}Al signals for the local complexes from the large scales of the Galactic plane by probing the latitudinal variation of ^{26}Al emission.

^{26}Al emission for low latitudes ($|b| < 5^\circ$) would be dominated by the large-scale origin in the Galactic disk. While ^{26}Al sources for high latitudes ($|b| > 5^\circ$) should originate from local star-formation systems in the Gould Belt. The Gould Belt appears as an ellipsoidal shaped ring with semi-major and minor axes equal to ~ 500 pc and 340 pc, respectively (Perrot & Grenier, 2003). The Sun is displaced from the center of the Gould Belt about 200 pc towards $l = 130^\circ$ (Guilout et al., 1998). The Vela region is located near the boundary of the Gould Belt towards $l \sim -90^\circ$. The nearby Sco-Cen region also belongs to the Gould Belt, extending from $(l, b) = (0^\circ, 20^\circ)$ towards $(l, b) = (-30^\circ, 0^\circ)$ (Sartori et al., 2003).

In Fig. 12, we present ^{26}Al spectra along Galactic latitudes for the 1st and 4th quadrants, respectively. No ^{26}Al signals are detected for two intermediate latitude regions of the 1st quadrant. While in the 4th quadrant, ^{26}Al emission is clearly detected in the latitude region of $5^\circ < b < 20^\circ$, which may originate toward the nearby Sco-Cen OB associations at a distance of ~ 140 pc. Additionally, a very weak ^{26}Al signal may be hinted toward the latitude region of $-60^\circ < l < 0^\circ$, $-20^\circ < b < -5^\circ$, which need a further check in future.

Finally, we determine the scale height of the Galactic plane in ^{26}Al emission by comparing the fit quality for sets of two different plausible geometrical models for the ^{26}Al source density distribution in the Galaxy (a Galactocentric double-exponential disk model (Wang et al., 2009) and a spiral-arm structure model based on Taylor & Cordes (1993), varying their scale height parameters). In order to avoid a bias from bright special regions such as Cygnus/Vela/Carina, we restrict this analysis to data within $|l| < 60^\circ$ and $|b| < 30^\circ$. Fig. 13 shows the variation of log-likelihood values with different scale heights for both model types. Here, the values for the exponential-disk models have been shifted by +16, as the spiral-arm model systematically provides a better description of our data. With $-2 \log L$ being asymptotically χ^2 distributed, we derive a scale height of 130_{-70}^{+120} pc (1σ) for the ^{26}Al emission in the inner Galactic disk, from the spiral arm model constraints. This confirms previous such studies based on COMPTEL data (Diehl et al., 1998).

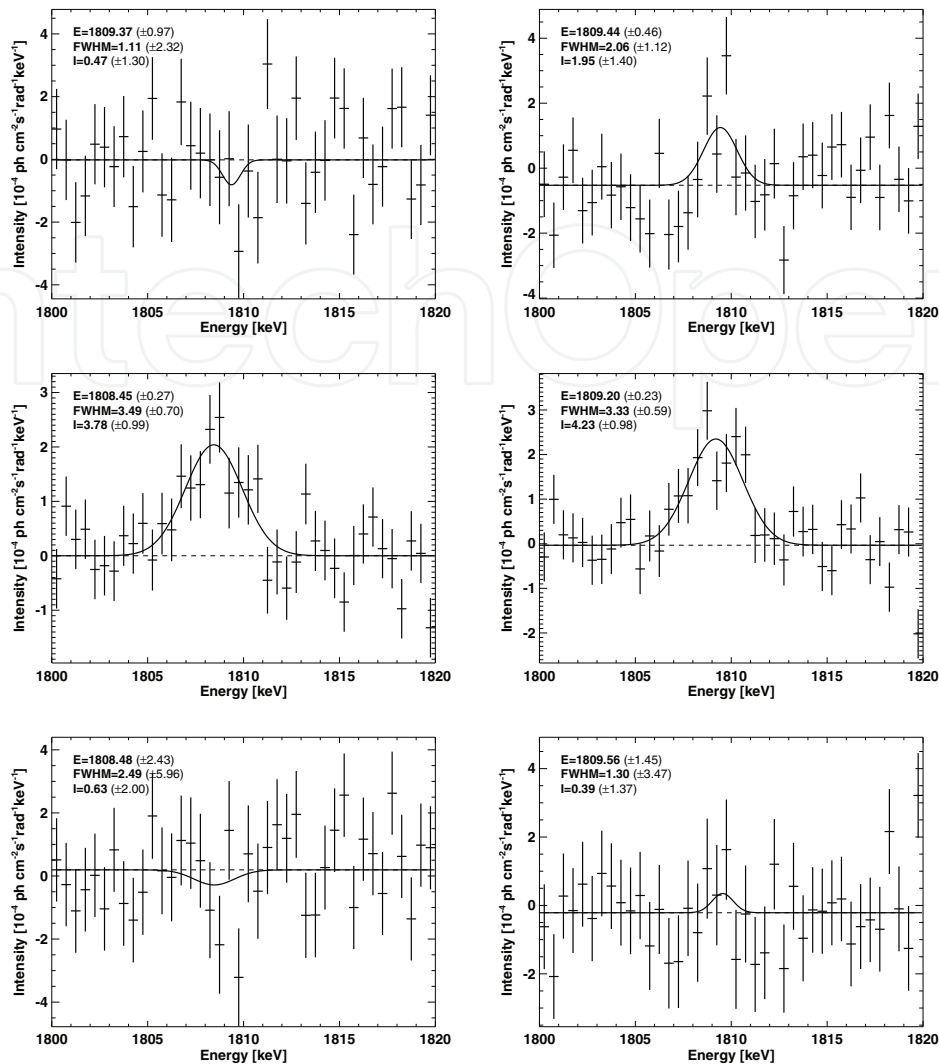


Fig. 12. ^{26}Al spectra for different latitude intervals of the 1st (left) and 4th (right) quadrants (taken from Wang, 2007): $5^\circ < b < 20^\circ$ (Top), $-5^\circ < b < 5^\circ$ (Middle), $-20^\circ < b < -5^\circ$ (Bottom).

4.5 ^{26}Al line shapes of the Cygnus and Sco-Cen regions

The COMPTEL 1809 keV all-sky map attributed to radioactive decay of Galactic ^{26}Al confirmed the diffuse emission along the inner Galaxy. Several significant features of the reconstructed intensity pattern are flux enhancements in the directions of nearby star-formation regions, e.g., the Cygnus region (del Rio et al., 1996), the Vela region (Diehl et al., 1995b), and a possible feature above the Galactic center which is attributed to the nearby Sco-Cen region. Detections of ^{26}Al in these regions strongly support the hypothesis of massive stars and their descendent supernovae being the dominant sources of interstellar ^{26}Al . ^{26}Al near these young populations may be located in the different medium environment from the large scales in inner Galaxy, e.g. high turbulent velocities of interstellar medium in these star-formation regions due to stellar winds and supernova explosions.

The INTEGRAL/SPI is a powerful spectrometer to probe the ^{26}Al line shapes. So spectral studies of ^{26}Al line in these star-formation regions can provide new information of ^{26}Al sources

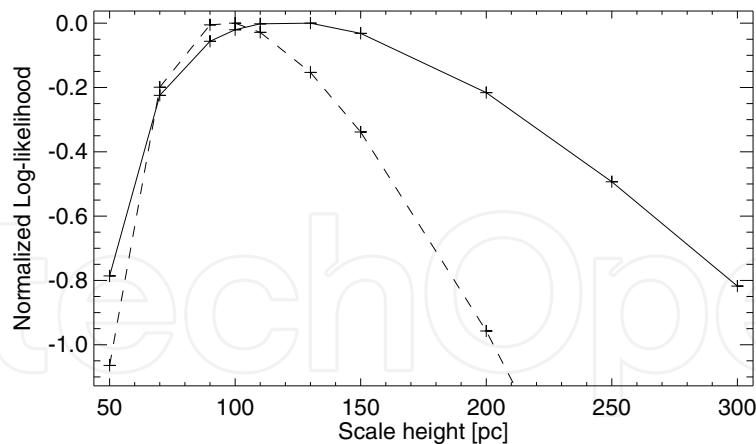


Fig. 13. Determination of the Galactic-disk scale height (from Wang et al., 2009). Shown is the logarithmic likelihood-ratio for the exponential-disk (dashed line) and spiral-arm structure models (solid line) for different scale height values. Log-likelihood values for the exponential-disk model have been offset by +16.

and their environments. In this section, we will show recent SPI results on ^{26}Al line shapes of two nearby star-formation regions: Cygnus and Sco-Cen.

4.5.1 Cygnus

The Cygnus region is one of the most active nearby star forming regions in the Galaxy with a mean age of ~ 3 Myr (Plüschke, 2001). The region as defined by the Cygnus 1.8 MeV emission feature contains numerous massive stars. The galactic O star catalogue lists 96 O stars in this field (Garmany et al., 1982). In addition, one finds 23 Wolf-Rayet stars in this region of which 14 are of WN-type, 8 of WC-type and one is classified as WO-star (van der Hucht, 2001). The Galactic SNR Catalogue lists 19 remnants in this region, for 9 of those age and distance have been estimated with sufficient accuracy (Green, 2011). Beside numerous open clusters, the region contains nine OB associations (Alter et al., 1970; Plüschke, 2001). Fig. 14 shows the distribution of O and WR stars, SNRs and OB associations in the direction of Cygnus as viewed from above the galactic plane. Therefore, the Cygnus region provides a good opportunity to study the physics of massive stars, specially on the nucleosynthesis processes which will enrich the interstellar medium with new elements.

The ^{26}Al emission from the Cygnus region was first reported by the COMPTEL imaging observations (see Fig. 5). With two years of COMPTEL data, del Rio et al. (1996) derived a flux of $(7.0 \pm 1.4) \times 10^{-5} \text{ph cm}^{-2} \text{s}^{-1}$ from a sky region defined as $73^\circ < l < 93^\circ$, $-9^\circ < b < 9^\circ$. Using 9 years of COMPTEL data, Plüschke (2001) found a flux of $(10.3 \pm 2.0) \times 10^{-5} \text{ph cm}^{-2} \text{s}^{-1}$ from a slightly larger region covering $70^\circ < l < 96^\circ$, $-9^\circ < b < 25^\circ$.

INTEGRAL/SPI has done deep surveys around the Cygnus region. ^{26}Al line shape of Cygnus has been detailedly studied by SPI. With early SPI data, the first result of ^{26}Al line emission from the Cygnus region showed a 1809 keV line flux of $(7.3 \pm 1.8) \times 10^{-5} \text{ph cm}^{-2} \text{s}^{-1}$ from a sky region defined as $73^\circ < l < 93^\circ$, $|b| < 9^\circ$ (Knödlseher et al., 2004). The ^{26}Al line from Cygnus appears moderately broadening, with an intrinsic FWHM of (3.3 ± 1.3) keV. Recently, new SPI results show the ^{26}Al flux of $\sim (7.2 \pm 1.2) \times 10^{-5} \text{ph cm}^{-2} \text{s}^{-1}$ for the region

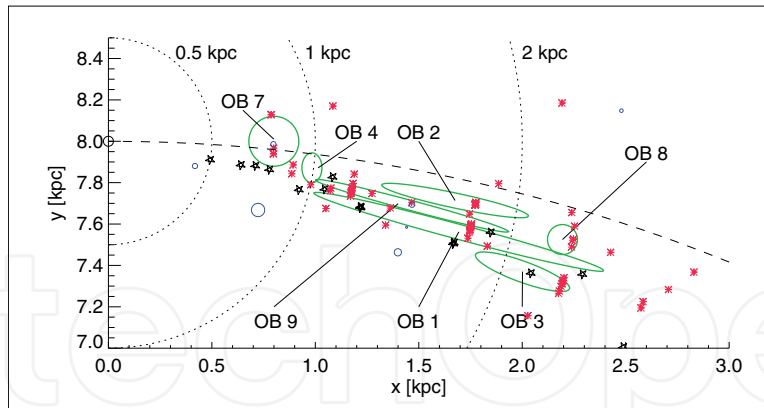


Fig. 14. Distribution of O and WR stars (red and black stars) as well as SNR (blue circles) and OB associations (green ellipses) in the direction of Cygnus as viewed from above the galactic plane (from Plüschke 2001). The sun is allocated along the y-axis at 8.0 kpc.

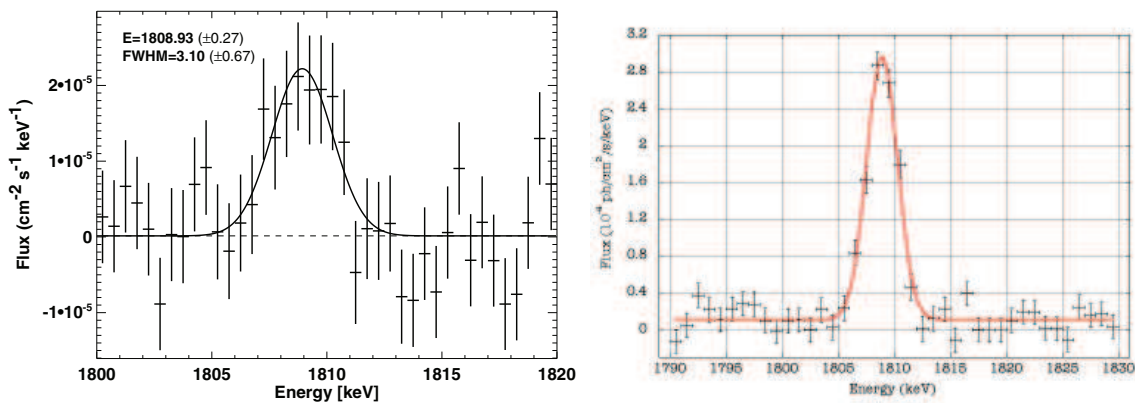


Fig. 15. Spectra of ^{26}Al line emission from the Cygnus region: left panel from Wang (2007); right one from Martin et al. (2009a). Both analyses show the ^{26}Al line flux around $(6 - 7) \times 10^{-5} \text{ ph cm}^{-2} \text{ s}^{-1}$ with a narrow line feature.

of $65^\circ < l < 95^\circ$, $-13^\circ < b < 17^\circ$ (Fig. 15 left panel), but found a narrow line feature with an intrinsic FWHM of $0.9 \pm 0.8 \text{ keV}$ (Wang 2007; 2008). The narrow line feature was confirmed by re-analysis SPI data by Martin et al. (2009), in which the ^{26}Al decay emission from Cygnus was represented as a $3^\circ \times 3^\circ$ Gaussian centred on $(l, b) = (81^\circ, 0.1^\circ)$, a position consistent with that of the massive Cyg OB2 cluster thought to dominate the energetics and nucleosynthesis of the Cygnus complex (Fig. 15 right panel). They obtained an ^{26}Al flux of $(6.0 \pm 1.0) \times 10^{-5} \text{ ph cm}^{-2} \text{ s}^{-1}$. In addition, they considered the possible Galactic background and foreground contributions, reducing the ^{26}Al flux of the Cygnus region to $\sim (3.9 \pm 1.1) \times 10^{-5} \text{ ph cm}^{-2} \text{ s}^{-1}$. This reduced ^{26}Al flux is comparable with the predicted one based on the latest models of stellar nucleosynthesis (Martin et al. 2010).

4.5.2 Sco-Cen

The nearest site of massive star formation, the Scorpius-Centaurus-Lupus region (hereafter the Sco-Cen region), is about 100 – 150 pc from the Sun. Nearby young stars are seen mostly in the Southern Hemisphere, which is related to recent massive star formation in Sco-Cen OB association that consists of three sub-regions: Upper Scorpius (US), Upper Centaurus Lupus

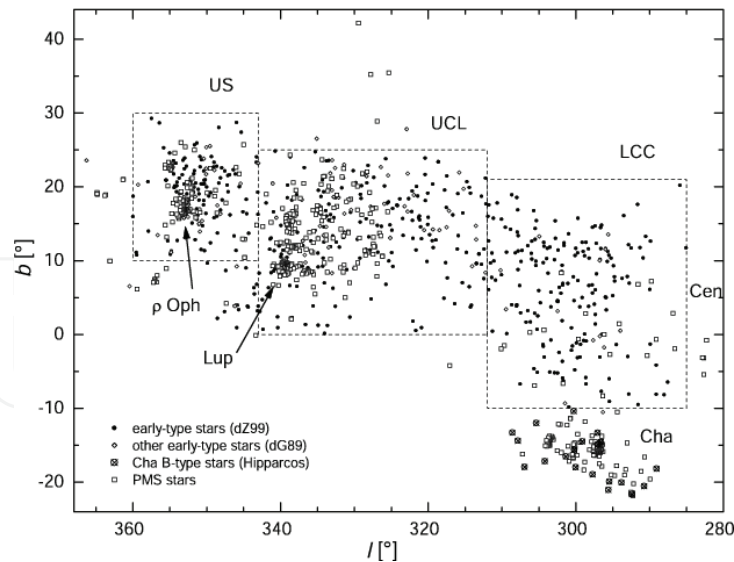


Fig. 16. Distribution of young stars including pre-main sequence stars (PMS) and young early-type stars in Sco-Cen region (from Sartori et al. 2003). Three sub-groups, UC, UCL and LCC are notified with the dashed-line boxes. The Chamaeleon OB association could be an extension of the Sco-Cen one. The positions of the rho Ophiuchus active star formation region and the Lupus cloud complex are also marked.

(UCL), and Lower Centaurus Crux (LCC), each distinguishable by different sky positions, age (de Geus et al., 1989), and kinematics (de Zeeuw et al. 1999, see Fig. 16).

The closest of the three sub-regions is Lower Centaurus-Crux (LCC) with an estimated distance of ~ 120 pc (de Zeeuw et al., 1999). The age of LCC is thought to be 10–20 Myr (de Geus et al., 1989). LCC is located toward the direction of the Galactic plane ($-70^\circ < l < -40^\circ$), and may contribute to ^{26}Al line emission observed by COMPTEL and SPI in the plane.

US and UCL are located at latitudes above the Galactic plane. The mean distance of UCL is ~ 140 pc, with an age of ~ 10 Myr (de Geus et al., 1989; de Zeeuw et al., 1999). UC is the youngest one with an age of $\sim 5 - 10$ Myr. Its mean distance is ~ 145 pc (de Geus et al., 1989; de Zeeuw et al., 1999). The rho Ophiuchus star forming region is located near the center of this group (Fig. 16). UC is just located in the direction above the Galactic centre ($l \sim -5^\circ, b \sim 18^\circ$), so the ^{26}Al emission structure in this direction observed by COMPTEL (Fig. 5) is most probably attributed to the UC OB association.

In Fig. 12, the significant excess of ^{26}Al emission in the intermediate latitudes $5^\circ < b < 20^\circ, l < 0^\circ$ suggests that this extra ^{26}Al emission should be attributed to nearby Sco-Cen OB associations. With more than 5 years of SPI observations, ^{26}Al gamma-ray signal toward Sco-Cen is detected with a significance level of $\sim 5\sigma$ (Diehl et al., 2010). The ^{26}Al line spectrum toward the Sco-Cen region is presented in Fig. 17. The observed flux of Sco-Cen is about $6 \times 10^{-5} \text{ph cm}^{-2} \text{s}^{-1}$ for the region of $12^\circ < b < 32^\circ, -16^\circ < l < -2^\circ$. This ^{26}Al flux corresponds to $1.1 \times 10^{-4} M_\odot$ at a distance of 150 pc. A typical ^{26}Al yield from a massive star in mass range $8-40 M_\odot$ is about $10^{-4} M_\odot$ (Limongi & Chieffi, 2006; Woosley & Heger, 2007), which is consistent with the derived ^{26}Al mass from observations. In Upper Sco, the most massive star is presumably a $50 M_\odot$ O5–O6 star, which may have exploded as a supernova about 1.5 Myr ago; the pulsar PSR J1932+1059 may be its compact remnant (Hoogerwerf et

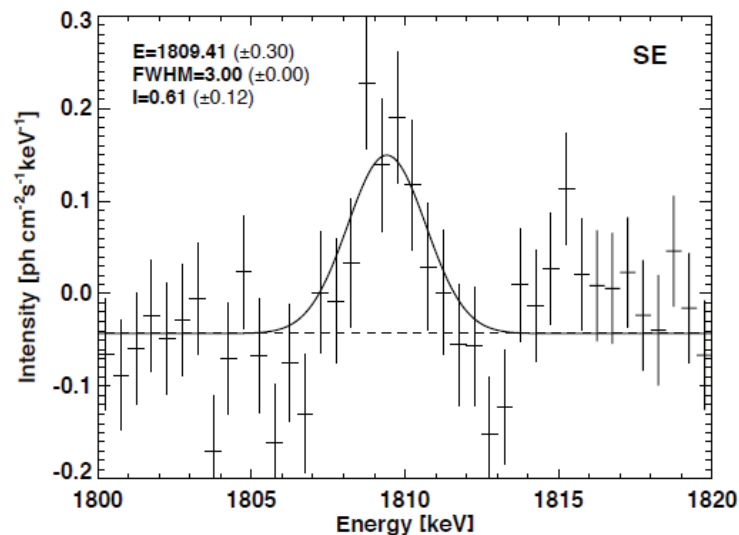


Fig. 17. ^{26}Al spectra for Sco-Cen by the 5-year SPI data. The ^{26}Al flux is derived as $F \sim (6.0 \pm 1.1) \times 10^{-5} \text{ ph cm}^{-2} \text{ s}^{-1}$ (from Diehl et al., 2010). A significant blueshift of line centroid energy is found.

al., 2000; Chatterjee et al., 2004). But because of uncertainty of this event and no obvious supernova activity being evident in Sco-Cen less than 1 My ago, the observed ^{26}Al could be a product of massive-star nucleosynthesis from a number of sources during an earlier epoch, rather than from a single event, like a supernova explosion.

The line width of ~ 3 keV is consistent with the instrumental line width of SPI at 1809 keV, implying no additional astrophysical line broadening in the Sco-Cen region. If we compare the centroid line energy with the ^{26}Al -decay laboratory value for the γ -ray energy of 1808.63 keV, a blueshift of 0.8 keV is evident. This blueshift suggests a kinematic Doppler effect from bulk motion of ^{26}Al ejecta corresponding to about 140 km s^{-1} toward us. The bulk motions of ^{26}Al ejecta in the Sco-Cen region suggest that the very nearby ^{26}Al sources have a quite different behavior in dynamics from the large scale feature in the inner Galaxy.

The origin of this bulk motions is still uncertain. The cavity surrounding Upper Sco appears to expand with a velocity of about $10 \pm 2 \text{ km s}^{-1}$, together with the relative motion of Sco-Cen stars with respect to the Sun of about 5 km s^{-1} , an approaching relative velocity of the entire complex is only few tens of km s^{-1} at most. But decaying ^{26}Al moves at higher velocities. So we exclude the association between the ^{26}Al decays and the cavity walls. The initial velocity of ^{26}Al ejecta from massive star winds and supernova explosion is about 1000 – 1500 km s^{-1} , which will slow down due to the interactions with the interstellar medium. Generally, if the medium is homogenous, the expanding ^{26}Al ejecta would be isotropic. In this case, the isotropic motions of ^{26}Al ejecta ($\sim 140 \text{ km s}^{-1}$) would induce a significant line broadening, but this Doppler broadening is not detected in SPI observations (Fig. 17). The possibility of inhomogenous ISM around the Sco-Cen region leads to the fast flowing ^{26}Al materials toward us. The other possibility is related to the assumed scenario that the ^{26}Al ejecta originated in Sco-Cen stream into the pre-blown cavity around it, decelerating through turbulence and interactions with the cavity walls (Diehl et al. 2010). The size of the cavity walls will be very large. Thus the whole ^{26}Al emission from the cavity walls is more extended on the sky. The detected region ($12^\circ < b < 32^\circ$, $-16^\circ < l < -2^\circ$) is small but bright compared with the total

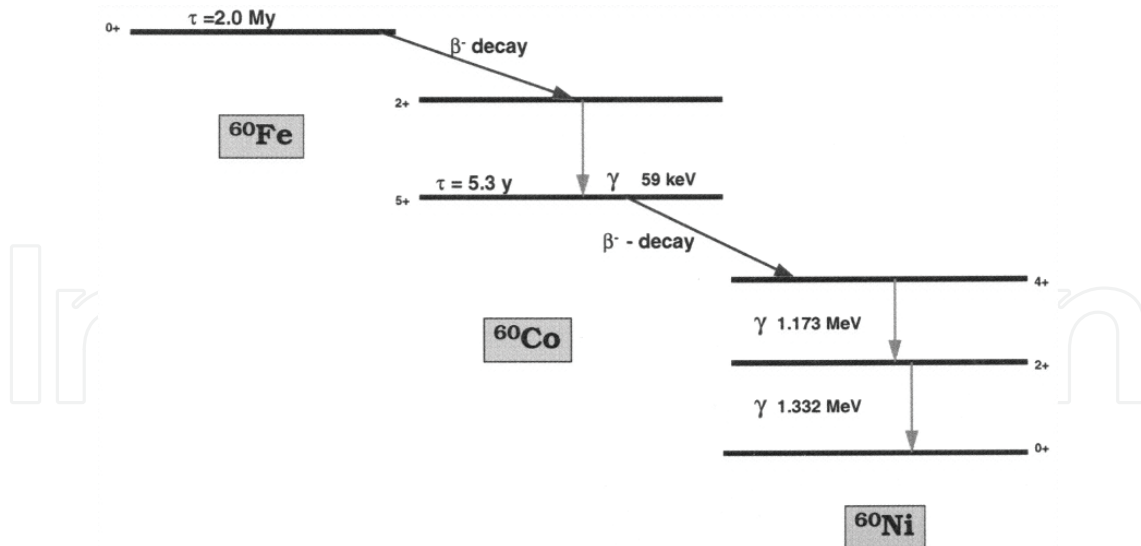


Fig. 18. The decay scheme of ^{60}Fe . The mean lifetime is about $(2 - 3) \times 10^6$ years. The gamma-ray flux at 59 keV line is $\sim 2\%$ of those at 1173 and 1332 keV.

extended ^{26}Al emission region. However, we cannot detect such more extended emission yet, both because it may be weaker than the main feature we show here, and because other locations of Sco-Cen stars overlap with Galactic-disk viewing directions.

5. Diffuse ^{60}Fe emission of the Galaxy

^{60}Fe is an unstable nucleus whose terrestrial half-life is $\simeq 1.5 \times 10^6$ years (recent measurements suggest a longer half-life time of $\sim 2.6 \times 10^6$ yr, Rugel et al. 2009), and it is located at the neutron rich side of the “valley of stable isotopes”. The ^{60}Fe isotope is synthesized in neutron capture reactions from the ^{56}Fe isotope which is abundant from former equilibrium nucleosynthesis of ^{56}Ni and its decay. Such *s*-process is expected to occur in stellar regions with efficient neutron-liberating reactions, e.g., ^{13}C and ^{20}Ne α captures, hence in the O/Ne burning shell and bottom of He burning shell of core-collapse supernovae, and the He burning shell inside massive stars.

The decay chains of ^{60}Fe are shown in Fig. 18. ^{60}Fe firstly decays to ^{60}Co , with emitting γ -ray photons at 59 keV, and then decays to ^{60}Ni , with emitting γ -ray photons at 1173 and 1332 keV. The gamma-ray efficiency of the 59 keV transition is only $\sim 2\%$ of those at 1173 and 1332 keV, so the gamma-ray flux at 59 keV is much lower than the fluxes of the high energy lines. The 59 keV gamma-ray line is very difficult to be detected with present missions. Measurements of the two high energy lines have been the main scientific target to study the radioactive ^{60}Fe isotope in the Galaxy.

^{60}Fe has been found to be part of meteorites formed in the early solar system (Shukolyukov & Lugmair, 1993). The inferred $^{60}\text{Fe}/^{56}\text{Fe}$ ratio for these meteorites exceeded the interstellar-medium estimates from nucleosynthesis models, which led to suggestion that the late supernova ejection of ^{60}Fe occurred before formation of the solar system (Tachibana & Huss, 2003; Tachibana et al., 2006). Yet, this is a proof for cosmic ^{60}Fe production, accelerator-mass spectroscopy of seafloor crust material from the southern Pacific ocean has revealed an ^{60}Fe excess in a crust depth corresponding to an age of 2.8 Myr (Knie et al., 2004). From this interesting measurement, it is concluded that a supernova explosion event

near the solar system occurred about 3 Myr ago, depositing some of its debris directly in the earth's atmosphere. All these measurements based on material samples demonstrate that ^{60}Fe nucleosynthesis does occur in nature. It is now interesting to search for current ^{60}Fe production in the Galaxy through detecting radioactive-decay γ -ray lines.

Many experiments and efforts were made to measure the ^{60}Fe gamma-ray emission. The first detection of ^{60}Fe lines was provided by HEAO-3, the ^{60}Fe flux from the inner Galaxy region ($-30^\circ < l < 30^\circ$) is $\sim (5.3 \pm 4.3) \times 10^{-5} \text{ ph cm}^{-2} \text{ s}^{-1} \text{ rad}^{-1}$ (Mahoney et al., 1982). The SMM Gamma-Ray Spectrometer reported a ^{60}Fe flux of $(2.9 \pm 2.5) \times 10^{-5} \text{ ph cm}^{-2} \text{ s}^{-1} \text{ rad}^{-1}$ (Leising & Share, 1994). OSSE aboard the COMPTON Observatory gave a ^{60}Fe flux of $(6.3 \pm 4.5) \times 10^{-5} \text{ ph cm}^{-2} \text{ s}^{-1} \text{ rad}^{-1}$ (Harris et al., 1994; 1997). And COMPTEL aboard the COMPTON Observatory also reported a ^{60}Fe flux limit of $1.2 \times 10^{-4} \text{ ph cm}^{-2} \text{ s}^{-1} \text{ rad}^{-1}$ (2σ , Diehl et al. 1997). The Gamma-Ray Imaging Spectrometer (GRIS) reported an upper limit for the ^{60}Fe flux of $6.8 \times 10^{-5} \text{ ph cm}^{-2} \text{ s}^{-1} \text{ rad}^{-1}$ (2σ , Naya et al. 1998). Recently, RHESSI reported observations of the gamma-ray lines from ^{60}Fe with a signal of 2.6σ significance, and an average flux of $(3.6 \pm 1.4) \times 10^{-5} \text{ ph cm}^{-2} \text{ s}^{-1}$ (Smith, 2004b) from the inner Galaxy.

The analysis of the first year of data from the SPI data resulted in a similarly marginally-significant detection of these γ -ray lines from ^{60}Fe ($\sim 3\sigma$, Harris et al. 2005), with an average line flux of $(3.7 \pm 1.1) \times 10^{-5} \text{ ph cm}^{-2} \text{ s}^{-1}$ from the inner Galaxy. With more than 3-year SPI data, we detected the diffuse ^{60}Fe emission in the Galaxy with a significance level of $\sim 5\sigma$ by superposing two gamma-ray lines at 1173 keV and 1332 keV (Fig. 19, Wang et al., 2007). Line energies of the ^{60}Fe lines in the laboratory are 1173.23 and 1332.49 keV. For this superposition, we therefore define the zero of the relative energy axis at 1173 and 1333 keV, to derive the summed spectrum of all ^{60}Fe signals. The line flux estimated from the combined spectrum is $(4.4 \pm 0.9) \times 10^{-5} \text{ ph cm}^{-2} \text{ s}^{-1} \text{ rad}^{-1}$.

We also done searching for the possible ^{60}Fe signal in nearby star-formation regions, like the Cygnus and Vela regions. Since the majority of Cygnus region star-clusters are young (~ 3 Myr), from population synthesis studies of the massive stars in the Cygnus region it has been suggested that the ^{60}Fe production is low, consistent with the small number of recent supernova events inferred for this region ($F(1173 \text{ keV}) \sim 2 \times 10^{-6} \text{ ph cm}^{-2} \text{ s}^{-1}$, see Knödlseeder et al., 2002). The Vela region including a core-collapse supernova remnant Vela SNR at $d \sim 250$ pc (Cha et al., 1999) should be a good candidate for gamma-ray line emission from ^{60}Fe . With the SPI data, no significant ^{60}Fe signal was detected in these regions with an upper limit of $\sim 1.1 \times 10^{-5} \text{ ph cm}^{-2} \text{ s}^{-1}$ (2σ) (Wang et al. 2007; Martin et al., 2009a).

6. The ratio of $^{60}\text{Fe}/^{26}\text{Al}$

^{26}Al and ^{60}Fe would share at least some of the same production sites, i.e. massive stars and supernovae (Timmes et al. 1995; Limongi & Chieffi 2006). In addition both are long-lived radioactive isotopes, so we have good reasons to believe their gamma-ray distributions are similar as well. Therefore we adopt the sky distribution of ^{26}Al gamma-rays as our best model for celestial ^{60}Fe gamma-ray distribution. And we use an ^{26}Al distribution obtained in direct observations, from the 9-year COMPTEL data (Plüschke et al., 2001).

Different theoretical models have predicted the ratio of $^{60}\text{Fe}/^{26}\text{Al}$ (Limongi & Chieffi, 2006; Prantzos, 2004; Timmes et al., 1995). Gamma-ray observations could detect these two isotopes and report the flux ratio of $^{60}\text{Fe}/^{26}\text{Al}$ which can be directly compared with theories. Therefore,

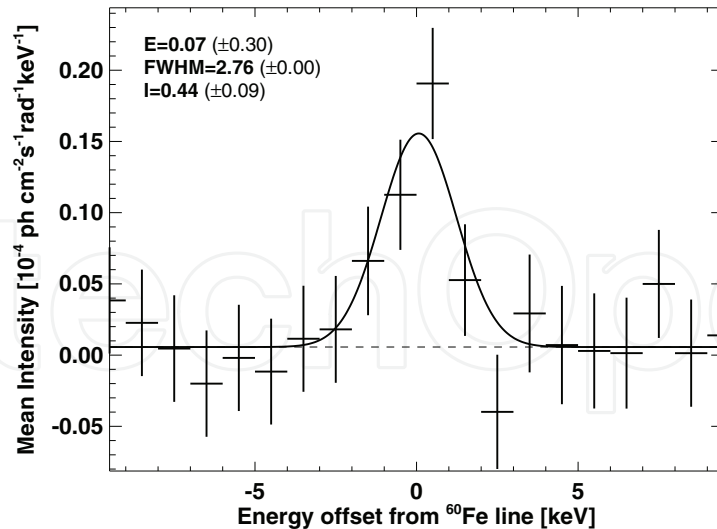


Fig. 19. The combined spectrum of the ^{60}Fe signal in the inner Galaxy by SPI, superimposing two gamma-ray lines (from Wang et al., 2007). In the laboratory, the line energies are 1173.23 and 1332.49 keV; here superimposed bins are zero at 1173 and 1332 keV. We find a detection significance of 4.9σ . The solid line represents a fitted Gaussian profile of fixed instrumental width (2.76 keV), and a flat continuum. The average line flux is estimated as $(4.4 \pm 0.9) \times 10^{-5} \text{ph cm}^{-2} \text{s}^{-1} \text{rad}^{-1}$.

Table 1. Different measurements of ^{60}Fe flux from the inner Galaxy and $^{60}\text{Fe}/^{26}\text{Al}$ flux ratio

Experiments	^{60}Fe flux ($10^{-5} \text{ph cm}^{-2} \text{s}^{-1} \text{rad}^{-1}$)	$F(^{60}\text{Fe})/F(^{26}\text{Al})$	references
HEAO-3	5.3 ± 4.3	0.09 ± 0.08	Mahoney et al. 1982
SMM	2.9 ± 2.5	0.1 ± 0.08	Leising & Share 1994
OSSE	6.3 ± 4.5	0.21 ± 0.15	Harris et al. 1997
COMPTEL	$< 12(2\sigma)$	0.17 ± 0.135	Diehl et al. 1997
GRIS	$< 6.8(2\sigma)$	$< 0.14(2\sigma)$	Naya et al. 1998
RHESSI	6.3 ± 5.0	0.16 ± 0.13	Smith 2004a
RHESSI	3.6 ± 1.4	0.10 ± 0.04	Smith 2004b
SPI	3.7 ± 1.1	0.11 ± 0.07	Harris et al. 2005
SPI	4.4 ± 0.9	0.148 ± 0.06	Wang et al. 2007

the measurement of the gamma-ray flux ratio $^{60}\text{Fe}/^{26}\text{Al}$ is important for discussions of the astrophysical origins of the two radioactive isotopes, and the nuclear physics involved in models for their production (addressing the uncertain nuclear reaction cross sections and half-lives).

Many experiments and efforts were made (see Table 1) to measure the $^{60}\text{Fe}/^{26}\text{Al}$ flux ratio that was predicted by theory – we now provide the most significant detection to date. In Figure 20, we show the previous constraints on the flux ratio of $^{60}\text{Fe}/^{26}\text{Al}$ together with the present SPI result, and compare the observational results with different theoretical predictions. The earliest observational limit was given from HEAO-3, $F(^{60}\text{Fe})/F(^{26}\text{Al}) = 0.09 \pm 0.08$, an upper limit being 0.27 (Mahoney et al., 1982) (in Fig. 20, we chose to give limits at 2σ for all reported

values below a significance of 3σ). Another limit was obtained with the SMM Gamma-Ray Spectrometer, a flux ratio of 0.1 ± 0.08 , the upper limit being ~ 0.27 (Leising & Share, 1994). OSSE aboard the COMPTON Observatory gave a flux ratio of 0.21 ± 0.15 , and the upper limit is ~ 0.51 (Harris et al., 1994; 1997). COMPTEL aboard the COMPTON Observatory also found ^{60}Fe gamma-rays, and reported a flux ratio value of $^{60}\text{Fe}/^{26}\text{Al}$ of 0.17 ± 0.135 , which translates into an upper limit ~ 0.44 (Diehl et al., 1997). The Gamma-Ray Imaging Spectrometer (GRIS) reported an upper limit for the ratio of < 0.14 (2σ , Naya et al. 1998). RHESSI has reported the first detection of ^{60}Fe gamma-ray lines, and gave a flux ratio 0.16 ± 0.13 for two-year data (Smith, 2004a). The first year data of SPI gave a flux ratio 0.11 ± 0.07 (Harris et al., 2005), and the present analysis of the 3-year SPI data finds a flux ratio 0.148 ± 0.06 (Wang et al. 2007).

Theoretical predictions of the ratio of $^{60}\text{Fe}/^{26}\text{Al}$ have undergone some changes since Timmes et al. (1995) published the first detailed theoretical prediction. In their paper, they combine a model for ^{26}Al and ^{60}Fe nucleosynthesis in supernova explosions with a model of chemical evolution, to predict that the steady production rates are $(2.0 \pm 1.0)M_{\odot} \text{ Myr}^{-1}$ for ^{26}Al , and $(0.75 \pm 0.4)M_{\odot} \text{ Myr}^{-1}$ for ^{60}Fe , which corresponds to a gamma-ray flux ratio $F(^{60}\text{Fe})/F(^{26}\text{Al}) = 0.16 \pm 0.12$. This prediction would be consistent with our present measurements. Since 2002, theoreticians have improved various aspects of the stellar-evolution models, including improved stellar wind models and the corresponding mass loss effects on stellar structure and evolution, of mixing effects from rotation, and also updated nuclear cross sections in the nucleosynthesis parts of the models. As a result, predicted flux ratios $^{60}\text{Fe}/^{26}\text{Al}$ rather fell into the range 0.8 ± 0.4 (see Prantzos 2004, based on, e.g. Rauscher et al. 2002, Limongi & Chieffi 2003) – such high values would be inconsistent with several observational limits and our SPI result. Recently, new ^{26}Al and ^{60}Fe yield models are presented (Limongi & Chieffi, 2006; Woosley & Heger, 2007), for stars of solar metallicity ranging in mass from $(11 - 120)M_{\odot}$. Limongi & Chieffi (2006) then combined their models of full stellar evolution up to and including the supernova with an adopted mass function to obtain a new prediction with latest nuclear reaction rate inputs. Their calculations yield a lower prediction for the $^{60}\text{Fe}/^{26}\text{Al}$ flux ratio of 0.185 ± 0.0625 , which is again consistent with the observational constraints (see Fig. 20).

In summary, uncertainties still exist, both in models and measurements of ^{60}Fe . On the theory side, stellar evolution in late stages is complex, nuclear reactions include neutron capture on unstable Fe isotopes, and explosive nucleosynthesis adds yet another complex ingredient. On the experimental side, the half-lives of ^{26}Al and ^{60}Fe , cosmic ray induced ^{60}Co radioactivity in the instrument and spacecraft and the limitations of spatial resolutions and sensitivity are issues reflected in the substantial uncertainties in experimental values. With more INTEGRAL/SPI data to come, and also with the development of next-generation gamma-ray spectrometers/telescopes, gamma-ray observations hopefully can help with an independent view on the astrophysical model components.

7. Summary and prospective

^{26}Al and ^{60}Fe have similar astrophysical origins in the Galaxy. Their nucleosynthesis and ejection into the interstellar medium are dominated by massive stars, their evolution, winds, and their subsequent core-collapse supernova explosions. With their much longer half-life (more than 1 million years), ^{26}Al and ^{60}Fe may propagate over significant distances of \simeq few hundred pc, and accumulates in the interstellar medium from many stars and supernovae until injection and β -decay are in balance in the ISM. ^{26}Al emission shows the diffuse

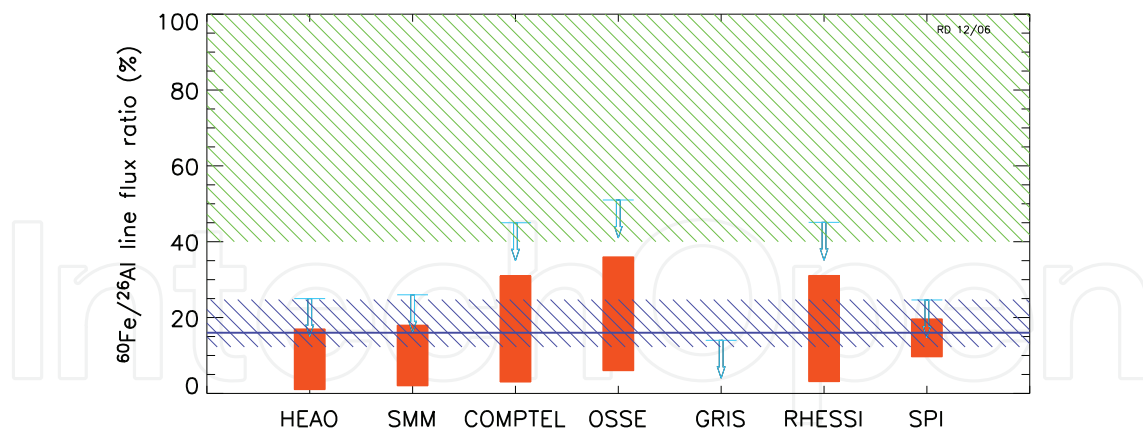


Fig. 20. Flux ratio of the gamma-ray lines from the two long-lived radioactive isotopes $^{60}\text{Fe}/^{26}\text{Al}$ from several observations, including our SPI result (also see Table 1; from Wang et al., 2007), with upper limits shown at 2σ for all reported values, and comparison with the recent theoretical estimates (the upper hatched region from Prantzos 2004; the horizontal line taken from Timmes et al. 1995; the lower hatched region, see Limongi & Chieffi 2006). The present SPI results find the line flux ratio to be $(14.8 \pm 6.0)\%$. Note that the primary instrument results on ^{60}Fe is compromised in the figure by different and uncertain ^{26}Al fluxes used for the $^{60}\text{Fe}/^{26}\text{Al}$ ratio.

Galaxy-wide feature which has been confirmed by the COMPTEL imaging observations, and Galactic ^{60}Fe emission may follow the similar diffuse distribution.

Diffuse γ -ray emissions from two long-lived radioactive isotopes ^{26}Al and ^{60}Fe in the Galaxy are significantly detected by the INTEGRAL/SPI. With high spectral resolution in MeV energy band, SPI has made the great progress on detecting diffuse ^{26}Al and ^{60}Fe emission and studying their line shapes. Details of line shapes help us to understand the dynamics of the ejected isotopes in the interstellar medium (e.g., nearby star formation regions) and in large scales of the Galaxy.

The new results on diffuse emissions of Galactic ^{26}Al and ^{60}Fe from more than five years of INTEGRAL/SPI observations and their astrophysical implications are briefly summarized here as follows:

(1) The study of the ^{26}Al line and its details in the large-scale of the Galaxy is one of the main goals of the SPI spectrometer on INTEGRAL. Using SPI data, we detect ^{26}Al γ -ray emission signal in the Galaxy with a significance level of $\sim 30\sigma$. The ^{26}Al flux integrated over the inner Galaxy of $(2.9 \pm 0.2) \times 10^{-4} \text{ ph cm}^{-2} \text{ s}^{-1} \text{ rad}^{-1}$. Taking the distance of the Sun to the Galactic center as $R_0 = 8.5 \text{ kpc}$, we convert the measured ^{26}Al flux to a Galactic ^{26}Al mass of $(2.6 \pm 0.6) M_\odot$. With detecting diffuse ^{26}Al emission in the Galaxy, we can also independently derive the core-collapse supernova rate of 1.9 ± 0.9 per century.

(2) The ^{26}Al line centroid energy appears blue-shifted relative to the laboratory value of $1808.65 \pm 0.07 \text{ keV}$ if integrated over the inner Galaxy ($\sim 1809.0 \pm 0.1 \text{ keV}$). With refined spatial resolution this turns out to be mostly due to asymmetric bulk motion which we find along the plane of the Galaxy, and attribute to asymmetries in inner spiral arms and to the Galaxy's bar.

- (3) The measured line width of ^{26}Al from the large-scale integrated inner Galaxy with an upper limit of 1.3 keV (2σ) is consistent with expectations from both Galactic rotation and modest interstellar-medium turbulence around the sources of ^{26}Al (turbulent velocities constrained below 160 km s^{-1} even when disregarding the effects of galactic rotation).
- (4) The brightness asymmetry of the ^{26}Al line emission for the 1st and 4th quadrants is discovered with a flux ratio of $F^{4\text{th}}/F^{1\text{st}} \sim 1.3$. The ^{26}Al emission asymmetry between fourth and first quadrant of the Galaxy seems to be lower than the intensity contrast of $1.8^{+0.5}_{-0.3}$ reported for positron annihilation emission from the disk of the Galaxy (Weidenspointner et al. 2008). ^{26}Al by itself releases a positron in 82% of its decays; it is uncertain, however, how this translates into annihilation photons, from the variety of slowing down and annihilation processes which determine the fate of positrons in interstellar space. Both spatial and temporal variations and non-linearities scaling with gas density may occur.
- (5) The study of ^{26}Al emission in spatially-restricted regions along the plane of the Galaxy found the ^{26}Al line centroid energy shifts along the Galactic plane: redshifts in the positive longitudes and blueshifts in the negative ones. The centroid line shift curve is consistent with the Galactic rotation curve. What's more, comparing the results for ^{26}Al ejecta velocity along the Galactic longitudes with other observations like HI, CO detections and theory still suggests that the hot gas (^{26}Al) undergoes additional acceleration in the direction of Galactic rotation (Fig. 11 bottom panel). Further analysis suggested that ^{26}Al velocity curves are incompatible with the circular orbits (Kretschmer, 2011). This implies that the Galactic bar would have a major influence on the kinematics of ^{26}Al ejecta in the inner Galaxy. Another possibility would be that ^{26}Al ejecta from the young star populations in molecular clouds would be emitted in the direction of Galactic rotation, possibly as a result of interaction with nearby clouds, thereby reaching the high radial velocities observed by SPI (Kretschmer, 2011).
- (6) The ^{26}Al line towards the direction of $20^\circ < l < 40^\circ$ shows a hint for additional line broadening. This line broadening may be attributed to the Aquila region which shows increased interstellar turbulence from stellar-wind and supernova activity at the characteristic age of stellar groups of that region, which may have created a supershell of substantial size ($320 \times 550 \text{ pc}$, see Maciejewski et al. 1996).
- (7) The scale height of Galactic-plane ^{26}Al emission is $130^{+120}_{-70} \text{ pc}$ (1σ), determined towards the inner Galaxy ($|l| < 60^\circ$). The scale height of Galactic ^{26}Al distributions is larger than the distributions of molecular clouds which is generally around 50 pc. However, this scale height is still significantly smaller than the "thick disk" part of the Galaxy. It is consistent with ^{26}Al being ejected from star-forming regions, and partly extending more towards the Galactic halo where gas pressure is lower than within the plane of the Galaxy ("champagne flows").
- (8) ^{26}Al emission brightness decreases significantly along the Galactic latitudes. But an additional ^{26}Al emission is discovered toward the intermediate latitude region of $5^\circ < b < 30^\circ$, $l < 0^\circ$. This component shows a hint for the ^{26}Al emission originated in nearby star-formation region Sco-Cen.
- (9) ^{26}Al line shapes from nearby star-formation regions (e.g., Cygnus and Sco-Cen) are obtained. The ^{26}Al line flux from the Cygnus region is $\sim 6 \times 10^{-5} \text{ ph cm}^{-2} \text{ s}^{-1}$, consistent with the previous COMPTEL result. No significant line broadening and shifts are detected. The Sco-Cen region is the nearest star-formation region. INTEGRAL/SPI first discovered the significant ^{26}Al line emission from this region and derived the ^{26}Al line shape. The ^{26}Al flux

from the Sco-Cen region is found to be $6 \times 10^{-5} \text{ ph cm}^{-2} \text{ s}^{-1}$. In addition a blueshift of ~ 0.8 keV for ^{26}Al line centroid energy was discovered. The blueshift suggested that the observed ^{26}Al ejecta in Sco-Cen have a bulk velocity of $\sim 140 \text{ km s}^{-1}$ toward us. The origin of the ^{26}Al ejecta bulk motions is still unknown, which would require more observational constraint.

(10) INTEGRAL/SPI first confirmed the existence of Galactic ^{60}Fe by detecting the γ -ray emission lines at 1173 and 1332 keV from the sky. ^{60}Fe signal was detected with a significance level of $\sim 5\sigma$ by combining the two γ -ray emission lines. The average line flux is derived to be $4.4 \times 10^{-5} \text{ ph cm}^{-2} \text{ s}^{-1}$.

(11) The flux ratio of $^{60}\text{Fe}/^{26}\text{Al}$ is derived to be $\sim 15\%$. This ratio provides a good constraint on the present nuclear reaction rate and massive star evolution models. There exist uncertainties in both observations and theories. On the theory side, stellar evolution in late stages is complex, nuclear reactions include neutron capture on unstable Fe isotopes, and explosive nucleosynthesis adds yet another complex ingredient. On the experimental side, half-lives of isotopes, cosmic ray induced ^{60}Co radioactivity in the instrument and spacecraft and the limitations of spatial resolutions and sensitivity are issues reflected in the substantial uncertainties in experimental values.

INTEGRAL still continues to accumulate the observational data for several years, with more exposure on the Galactic plane, covering more sky regions, specially in the intermediate latitudes. The deeper observations along the Galactic plane will increase the significance of the present results on ^{26}Al and ^{60}Fe . The further studies with high-resolution ^{26}Al line shapes will help to better understand the properties of ISM near groups of massive stars, and the bulk motion of gas in the inner Galaxy from Galactic rotation and other peculiar kinematics. The possible detection of ^{60}Fe signal variations along the Galactic plane can be carried out with nearly ten years of INTEGRAL/SPI data. Nearby ^{26}Al sources may be also discriminated with better exposure towards candidate sky regions, improving our determination of the ^{26}Al mass in the Galaxy and towards regions where the stellar census is known to a better degree. Studies of ^{26}Al from nearby star-formation regions (e.g., Cygnus, Vela, Sco-Cen, Orion) are a promising diagnostic for the massive star origin of Galactic ^{26}Al and kinematics of ^{26}Al ejecta in ISM. Presently ^{26}Al line shapes are derived only in two nearby regions Cygnus and Sco-Cen. The ^{26}Al emission signal from Vela and Orion regions and their line shapes would be studied with INTEGRAL/SPI. These studies will provide the important constraints on the nucleosynthesis of supernovae and massive stars.

SPI aboard INTEGRAL has a high spectral resolution but still a very limited sensitivity over 0.1 – 8 MeV, e.g., ^{26}Al emission can be only detected in the inner Galaxy and nearby star-formation regions, but no signal is detected from individual sources, like supernova remnants. The MeV gamma-ray astronomy retards for a long time for the lack of a sensitive instrument from 0.1 – 10 MeV compared to the present keV and GeV band instruments (Chandra, XMM-Newton, Fermi/LAT). Therefore, the development of the next-generation MeV gamma-ray telescope is very necessary and urgent in multi-wavelength instrument sensitivity for full understanding of the high energy astrophysics, specially in the new observational window for the nuclear radioactivity gamma-ray line emissions, e.g., ^{26}Al , ^{60}Fe , ^{44}Ti , ^{56}Co and 511 keV annihilation line (also see Fig. 21). The potential γ -ray line sources: the 511 keV line from Galactic novae and nearby supernova remnants; ^{60}Fe from the Vela SNR; ^{56}Co from SN Ia at a distance up to 80 Mpc; ^{44}Ti from more young SNRs, e.g. Tycho, Kepler, SN 1987A; ^{26}Al from individual sources, like the Vela SNR, the closest Wolf-Rayet star WR

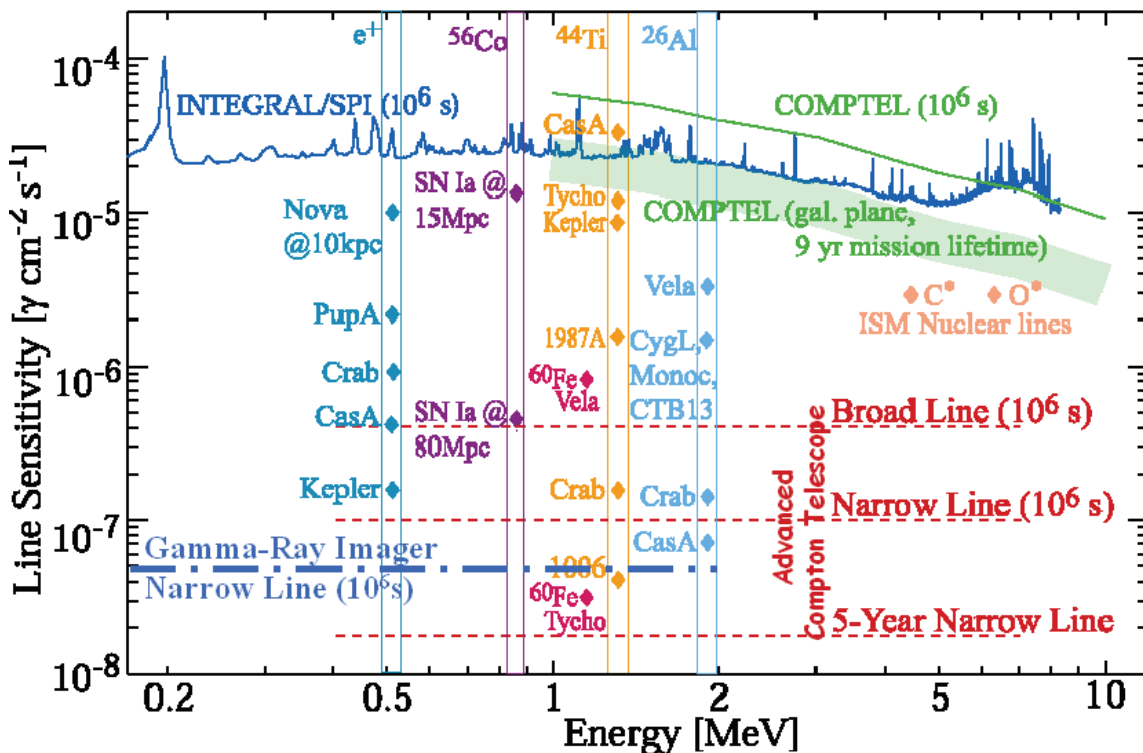


Fig. 21. Future goals for γ -ray line astronomy (0.2 – 10 MeV): possible next-generation instruments (e.g., Advanced-Compton Telescope, Gamma-Ray Imager) and potential candidate γ -ray line sources for e^-e^+ annihilation line, ^{56}Co , ^{44}Ti , ^{60}Fe and ^{26}Al (from Boggs et al. 2003). Sensitivities of SPI and COMPTEL are also shown here for comparison.

11 in the Vela star-formation region, even from Crab and Cas A; and the nuclear exciting lines in ISM from C and O, are well below the sensitivity limits of present missions, but could be detected by the future advanced γ -ray telescopes, i.e., visionary Advanced Compton Telescope (ACT) and European Gamma-Ray Imager (GRI) mission. Detections of the 511 keV line, ^{44}Ti , ^{26}Al and ^{60}Fe from some individual SNRs will put the connection with yields of these radioactivity isotopes from stellar nucleosynthesis on solid ground. Era for accurate γ -ray line astronomy and nuclear astrophysics may come near with the launch of next-generation MeV γ -ray missions.

8. Acknowledgments

The author thanks the book editor for inviting me to write a book chapter in addressing the issues of long-lived radioactivity isotopes in the Galaxy. This work is based on observations of INTEGRAL, an ESA project with instrument and science data center funded by ESA member states (principle investigator countries: Denmark, France, Germany, Italy, Switzerland and Spain), the Czech Republic and Poland, and with participation of Russia and US. We are also grateful to the support by the National Natural Science Foundation of China under grants 10803009, 10833003, 11073030.

9. References

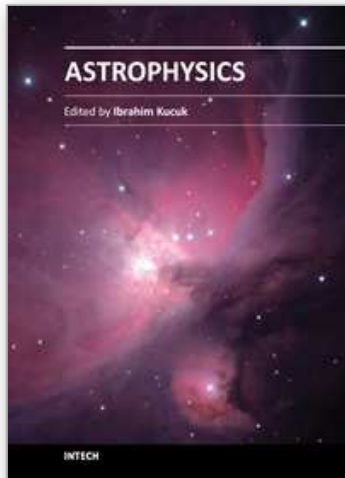
Alter, G. and Balazs, B. and Ruprecht, J. and Vanysek, J. (1970). Catalogue of star clusters and associations, Budapest: Akademiai Kiado, 2nd ed., edited by G. Alter, B. Balazs,

- J. Ruprecht
- Arnett, W. D. (1977). Eight Texas Symposium on Relativistic Astrophysics, Papagiannis, M. D., ed., 90
- Bloemen, H. et al. (1994). *Astrophysical Journal Supplements*, Vol. 92, 419-423
- Boggs, S. E. et al. (2003). *X-Ray and Gamma-Ray Telescopes and Instruments for Astronomy, Proceedings of the Society of Photo-Optical Instrumentation Engineers (SPIE) Conference*, Truemper, J. E. and Tananbaum, H. D. ed., Vol. 4851, 1221-1227
- Brandt, J. C. (1969). *Solar Physics*, Vol. 6, 171
- Brand, J. and Blitz, L. (1993). *Astronomy & Astrophysics*, Vol. 275, 67
- Burbidge, E. M., Burbidge, G. R., Fowler, W. A. and Hoyle, F. (1957). Synthesis of the Elements in Stars, *Reviews of Modern Physics*, Vol. 29, Issue 4, 547-650
- Caughlan, G. R. and Fowler, W. A. (1988). *Atomic Data and Nuclear Data Tables*, Vol. 40, 283
- Cha, A. N. and Sembach, K. R. and Danks, A. C. (1999). *Astrophysical Journal Letters*, Vol. 515, L25-L28
- Chatterjee, S. et al. (2004). Pulsar Parallaxes at 5 GHz with the Very Long Baseline Array, *Astrophysical Journal*, Vol. 604, 339-345
- Chen, W. and Diehl, R. and Gehrels, N. and Hartmann, D. and Leising, M. and Naya, J. E. and Prantzos, N. and Tueller, J. and von Ballmoos, P. (1997). ESA SP-382: The Transparent Universe, Winkler, C. and Courvoisier, T. J.-L. and Durouchoux, P., ed., 105
- Clayton, D. D. & Leising, M. D. (1987). ^{26}Al in the interstellar medium, *Physics Report*, Vol. 144, 1-50
- Clayton, D. D. (1994). *Nature*, Vol. 368, 222
- de Geus, E. J. and de Zeeuw, P. T. and Lub, J. (1989). *Astronomy & Astrophysics*, Vol. 216, 44-61
- del Rio, E. et al. (1996). *Astronomy & Astrophysics*, Vol. 315, 237-242
- de Zeeuw, P. T. and Hoogerwerf, R. and de Bruijne, J. H. J. and Brown, A. G. A. and Blaauw, A. (1999). *Astronomical Journal*, Vol. 117, 354-399
- Diehl, R. et al. (1995a). *Astronomy & Astrophysics*, Vol. 298, 445
- Diehl, R. et al. (1995b). *Astronomy & Astrophysics*, Vol. 298, L25-L28
- Diehl, R. et al. (1997). AIP Conf. Proc. 410: Proceedings of the Fourth Compton Symposium, Dermer, C. D. and Strickman, M. S. and Kurfess, J. D. ed., 1109
- Diehl, R. et al. (1998). IAU Colloq. 166, D. Breitschwerdt, M. J. Freyberg and J. Truemper, ed., *Lecture Notes in Physics*, Berlin Springer Verlag, 506, 393
- Diehl, R. and Timmes, F. X. (1998). *Gamma-Ray Line Emission from Radioactive Isotopes in Stars and Galaxies The Publications of the Astronomical Society of the Pacific*, Vol. 110, 637-659
- Diehl, R. and Halloin, H. and Kretschmer, K. and Lichti, G. G. and Schönfelder, V. and Strong, A. W. and von Kienlin, A. and Wang, W. and Jean, P. and Knödlseher, J. and Roques, J.-P. and Weidenspointner, G. and Schanne, S. and Hartmann, D. H. and Winkler, C. and Wunderer, C. (2006a). *Nature*, Vol. 439, 45-47
- Diehl, R. and Halloin, H. and Kretschmer, K. and Strong, A. W. and Wang, W. and Jean, P. and Lichti, G. G. and Knödlseher, J. and Roques, J.-P. and Schanne, S. and Schönfelder, V. and von Kienlin, A. and Weidenspointner, G. and Winkler, C. and Wunderer, C. (2006b). *Astronomy & Astrophysics*, Vol. 449, 1025-1031
- Diehl, R.; Lang, M. G.; Martin, P.; Ohlendorf, H.; Preibisch, Th.; Voss, R.; Jean, P.; Roques, J.-P.; von Ballmoos, P.; Wang, W. (2010). Radioactive ^{26}Al from the Scorpius-Centaurus association, *Astronomy & Astrophysics*, Vol. 522, 51

- Durouchoux, P. et al. (1993). *Astrophysics & Space Science*, Vol. 97, 185-187
- Gamow, G. (1946). *Expanding Universe and the Origin of Elements*, *Physical Review*, Vol. 70, 572-573
- Garmany, C. D. and Conti, P. S. and Chiosi, C. (1982). *Astrophysical Journal*, Vol. 263, 777-790
- Gehrels, N. and Chen, W. (1996). *Astronomy & Astrophysics Supplements*, Vol. 120, 331
- Green, D. A. (2011). *Catalogue of Galactic Supernova Remnants*, URL: "<http://www.mrao.cam.ac.uk/surveys/snrs/>"
- Guillout, P. and Sterzik, M. F. and Schmitt, J. H. M. M. and Motch, C. and Neuhaeuser, R. (1998). *Astronomy & Astrophysics*, Vol. 337, 113-124
- Harris, M. J. et al. (1994). *Bulletin of the American Astronomical Society*, 968
- Harris, M. J. et al. (1997). *AIP Conf. Proc.* 410: *Proceedings of the Fourth Compton Symposium*, Dermer, C. D. and Strickman, M. S. and Kurfess, J. D. ed., 1079
- Harris, M. J. et al. (2005). *Astronomy & Astrophysics*, Vol. 433, L49-L52
- Hillebrandt, W. and Thielemann, F.-K. (1982). *Astrophysical Journal*, Vol. 255, 617-623
- Hoogerwerf, R.; de Bruijne, J. H. J.; de Zeeuw, P. T. (2000). *The Origin of Runaway Stars*, *Astrophysical Journal Letters*, Vol. 544, L133-L136
- Iyudin, A. F. and Diehl, R. and Bloemen, H. and Hermsen, W. and Lichti, G. G. and Morris, D. and Ryan, J. and Schoenfelder, V. and Steinle, H. and Varendorff, M. and de Vries, C. and Winkler, C. (1994). *Astronomy & Astrophysics*, Vol. 284, L1-L4
- Jensen, P. L. and Clausen, K. and Cassi, C. and Ravera, F. and Janin, G. and Winkler, C. and Much, R. (2003). *Astronomy & Astrophysics*, Vol. 411, L7-L17
- Jose, J. and Hernanz, M. and Coc, A. (1997). *Astrophysical Journal Letters*, Vol. 479, L55-L58
- Karakas, A. I. and Lattanzio, J. C. (2003). *Publications of the Astronomical Society of Australia*, Vol. 20, 279-293
- Knie, K. and Korschinek, G. and Faestermann, T. and Dorfi, E. A. and Rugel, G. and Wallner, A. (2004). *Physical Review Letters*, Vol. 93, 171103
- Knödseder, J. (1999). *Astrophysical Journal*, Vol. 510, 915-929
- Knödseder, J. and Cerviño, M. and Le Duigou, J.-M. and Meynet, G. and Schaerer, D. and von Ballmoos, P. (2002). *Astronomy & Astrophysics*, Vol. 390, 945-960
- Knödseder, J. et al. (2004). *ESA SP-552: 5th INTEGRAL Workshop on the INTEGRAL Universe*, Schoenfelder, V. and Lichti, G. and Winkler, C. ed., 33
- Kretschmer, K. and Diehl, R. and Hartmann, D. H. (2003). *Astronomy & Astrophysics*, Vol. 412, L47-L51
- Kretschmer, K. (2011). PhD Thesis, Technische Universität München
- Langer, N. (1989). *Astronomy & Astrophysics*, Vol. 220, 135-143
- Langer, N. and Braun, H. and Fliegner, J. (1995). *Astrophysics & Space Science*, Vol. 224, 275-278
- Leising, M. D. and Share, G. H. (1994). *Astrophysical Journal*, Vol. 424, 200-207
- Limongi, M. and Chieffi, A. (2006). *Astrophysical Journal*, Vol. 647, 483-500
- Maciejewski, W. et al. (1996). *Astrophysical Journal*, Vol. 469, 238
- Mahoney, W. A. and Ling, J. C. and Jacobson, A. S. and Lingenfelter, R. E. (1982). *Astrophysical Journal*, Vol. 262, 742
- Mahoney, W. A. and Ling, J. C. and Wheaton, W. A. and Jacobson, A. S. (1984). *Astrophysical Journal*, Vol. 286, 578-585
- Martin, P.; Knödseder, J.; Diehl, R.; Meynet, G. (2009). *New estimates of the gamma-ray line emission of the Cygnus region from INTEGRAL/SPI observations*, *Astronomy & Astrophysics*, Vol. 506, 703-710

- Martin, P.; Knödlseeder, J.; Meynet, G.; Diehl, R. (2010). Predicted gamma-ray line emission from the Cygnus complex, *Astronomy & Astrophysics*, Vol. 511, 86
- McKee, C. F. and Williams, J. P. (1997). *Astrophysical Journal*, Vol. 476, 144
- Meynet, G. and Arnould, M. and Prantzos, N. and Paulus, G. (1997). *Astronomy & Astrophysics*, Vol. 320, 460-468
- Miller, G. E. and Scalo, J. M. (1979). *Astrophysical Journal Supplements*, Vol. 41, 513-547
- Mowlavi, N. and Meynet, G. (2000). *Astronomy & Astrophysics*, Vol. 361, 959-976
- Naya, J. E. et al. (1998). Gamma-Ray Limits on Galactic ^{60}Fe Nucleosynthesis and Implications on the Origin of the ^{26}Al Emission, *Astrophysical Journal Letters*, Vol. 499, L169-L172
- Nofar, I. and Shaviv, G. and Starrfield, S. (1991). *Astrophysical Journal*, Vol. 369, 440-450
- Nugis, T. and Lamers, H. J. G. L. M. (2000). *Astronomy & Astrophysics*, Vol. 360, 227-244
- Oberlack, U. et al. (1996). *Astronomy & Astrophysics Supplements*, Vol. 120, 311
- Palacios, A. and Meynet, G. and Vuissoz, C. and Knödlseeder, J. and Schaerer, D. and Cerviño, M. and Mowlavi, N. (2005). *Astronomy & Astrophysics*, Vol. 429, 613-624
- Perrot, C. A. and Grenier, I. A. (2003). *Astronomy & Astrophysics*, Vol. 404, 519-531
- Plüschke, S. (2001). PhD Thesis, Technische Universität München
- Plüschke, S. and Diehl, R. and Schönfelder, V. and Bloemen, H. and Hermsen, W. and Bennett, K. and Winkler, C. and McConnell, M. and Ryan, J. and Oberlack, U. and Knödlseeder, J. (2001). *ESA SP-459: Exploring the Gamma-Ray Universe*, Gimenez, A. and Reglero, V. and Winkler, C. ed., 55-58
- Prantzos, N. and Diehl, R. (1996). Radioactive ^{26}Al in the galaxy: observations versus theory, *Physics Reports*, Vol. 267, 1-69
- Prantzos, N. (2004). *Astronomy & Astrophysics*, Vol. 420, 1033-1037
- Purcell, W. R. and Cheng, L.-X. and Dixon, D. D. and Kinzer, R. L. and Kurfess, J. D. and Leventhal, M. and Saunders, M. A. and Skibo, J. G. and Smith, D. M. and Tueller, J. (1997). *Astrophysical Journal*, Vol. 491, 725
- Ramaty, R. and Lingenfelter, R. E. (1977), *Astrophysical Journal Letters*, Vol. 213, L5-L7
- Ramaty, R. (1996). *Astrophysics & Space Science*, Vol. 120, 373
- Ramaty, R. and Lingenfelter, R. E. (1979). *Nature*, 278, 127-132
- Rauscher, T. and Heger, A. and Hoffman, R. D. and Woosley, S. E. (2002). *Astrophysical Journal*, Vol. 576, 323-348
- Reed, B. C. (2005). *Astronomical Journal*, Vol. 130, 1652-1657
- Rice, E. L., Prato, L. & McLean, I. S. 2006, *Astrophysical Journal*, Vol. 647, 432
- Rolfs, C. E. and Rodney, W. S. (1994). *Cauldrons in the Cosmos*, University of Chicago Press
- Rugel, G.; Faestermann, T.; Knie, K.; Korschinek, G.; Poutivtsev, M.; Schumann, D.; Kivel, N.; Günther-Leopold, I.; Weinreich, R.; Wohlmuther, M. (2009). *Physical Review Letters*, Vol. 103, Issue 7, id. 072502
- Sartori, M. J. and Lépine, J. R. D. and Dias, W. S. (2003). *Astronomy & Astrophysics*, Vol. 404, 913-926
- Schoenfelder, V. and Varendorff, M. (1991). *AIP Conf. Proc. 232: Gamma-Ray Line Astrophysics*, Durouchoux, P. and Prantzos, N. ed., 101-115
- Schoenfelder, V. et al. (1993). *Astrophysical Journal Supplements*, Vol. 86, 657-692
- Share, G. H. and Kinzer, R. L. and Kurfess, J. D. and Forrest, D. J. and Chupp, E. L. and Rieger, E.. (1985). *Astrophysical Journal Letters*, Vol. 292, L61-L65
- Shukolyukov, A. and Lugmair, G. W. (1993). *Science*, Vol. 259, 1138-1142
- Smith, D. M. (2003). *Astrophysical Journal Letters*, Vol. 589, L55-L58
- Smith, D. M. (2004a). *New Astronomy Review*, Vol. 48, 87-91

- Smith, D. M. (2004b). ESA SP-552: 5th INTEGRAL Workshop on the INTEGRAL Universe, Schoenfelder, V. and Lichti, G. and Winkler, C. ed., 45
- Tachibana, S. and Huss, G. R. (2003). *Astrophysical Journal Letters*, Vol. 588, L41-L44
- Tachibana, S. and Huss, G. R. and Kita, N. T. and Shimoda, G. and Morishita, Y. (2006). *Astrophysical Journal Letters*, Vol. 639, L87-L90
- Taylor, J. H. and Cordes, J. M. (1993). *Astrophysical Journal*, Vol. 411, 674-684
- Thielemann, F.-K. and Nomoto, K. and Hashimoto, M.-A. (1996). *Astrophysical Journal*, Vol. 460, 408
- Timmes, F. X. and Woosley, S. E. and Hartmann, D. H. and Hoffman, R. D. and Weaver, T. A. and Matteucci, F. (1995). *Astrophysical Journal*, Vol. 449, 204
- Ubertini, P. et al. (2003). *Astronomy & Astrophysics*, Vol. 411, L131-L139
- van der Hucht, K. A. and Hidayat, B. and Admiranto, A. G. and Supelli, K. R. and Doom, C. (1988). *Astronomy & Astrophysics*, Vol. 199, 217-234
- van der Hucht, K. A. (2001). The VIIth catalogue of galactic Wolf-Rayet stars, *New Astronomy Review*, Vol. 45, 135-232
- Vedrenne, G. et al. (2003). *Astronomy & Astrophysics*, Vol. 411, L63-L70
- von Ballmoos, P. and Diehl, R. and Schoenfelder, V. (1987). *Astrophysical Journal*, Vol. 318, 654-663
- Wallerstein, G. et al. (1997). Synthesis of the elements in stars: forty years of progress, *Reviews of Modern Physics*, Vol. 69, Issue 4, 995-1084
- Wang, W. (2007). PhD Thesis, Technische Universität München
- Wang, W. et al. (2007). SPI observations of the diffuse ^{60}Fe emission in the Galaxy, *Astronomy & Astrophysics*, Vol. 469, 1005-1012
- Wang, W. (2008). Study of Long-lived Radioactive Sources in the Galaxy with INTEGRAL/SPI, *Publications of the Astronomical Society of the Pacific*, Vol. 120, 118-119
- Wang, W. et al. (2009). Spectral and intensity variations of Galactic ^{26}Al emission, *Astronomy & Astrophysics*, Vol. 496, 713-724
- Ward, R. A. and Fowler, W. A. (1980). *Astrophysical Journal*, Vol. 238, 266-286
- Weaver, T. A. and Woosley, S. E. (1993). *Physics Reports*, Vol. 227, 65-96
- Weidenspointner, G. et al. (2008). *Nature*, Vol. 451, 159
- Weiss, A. and Truran, J. W. (1990). *Astronomy & Astrophysics*, Vol. 238, 178-186
- Wiescher, M. and Gorres, J. and Thielemann, F.-K. and Ritter, H. (1986). *Astronomy & Astrophysics*, Vol. 160, 56-72
- Winkler, C. et al. (2003). *Astronomy & Astrophysics*, Vol. 411, L1-L6
- Woosley, S. E. and Weaver, T. A. (1980). *Astrophysical Journal*, Vol. 238, 1017-1025
- Woosley, S. E. (1986). Saas-Fee Advanced Course 16: Nucleosynthesis and Chemical Evolution, Audouze, J. and Chiosi, C. and Woosley, S. E., ed., 1
- Woosley, S. E., Hartmann, D. H., Hoffman, R. D. and Haxton, W. C. (1990). *Astrophysical Journal*, Vol. 356, 272-301
- Woosley, S. E. and Weaver, T. A. (1995). *Astrophysical Journal Supplements*, Vol. 101, 181
- Woosley, S. E. (1997). *Astrophysical Journal*, Vol. 476, 801
- Woosley, S. E. & Heger, A. (2007). Nucleosynthesis and remnants in massive stars of solar metallicity, *Physics Reports*, Volume 442, Issue 1-6, p. 269-283



Astrophysics

Edited by Prof. Ibrahim Kucuk

ISBN 978-953-51-0473-5

Hard cover, 398 pages

Publisher InTech

Published online 30, March, 2012

Published in print edition March, 2012

This book provides readers with a clear progress to theoretical and observational astrophysics. It is not surprising that astrophysics is continually growing because very sophisticated telescopes are being developed and they bring the universe closer and make it accessible. Astrophysics Book presents a unique opportunity for readers to demonstrate processes do occur in Nature. The unique feature of this book is to cover different aspects in astrophysics covering the topics: • Astronomy • Theoretical Astrophysics • Observational Astrophysics • Cosmology • The Solar System • Stars • Planets • Galaxies • Observation • Spectroscopy • Dark Matter • Neutron Stars • High Energy Astrophysics

How to reference

In order to correctly reference this scholarly work, feel free to copy and paste the following:

Wei Wang (2012). Diffuse Emission of ^{26}Al and ^{60}Fe in the Galaxy, Astrophysics, Prof. Ibrahim Kucuk (Ed.), ISBN: 978-953-51-0473-5, InTech, Available from: <http://www.intechopen.com/books/astrophysics/diffuse-emission-of-26al-and-60fe-in-the-galaxy>

INTECH
open science | open minds

InTech Europe

University Campus STeP Ri
Slavka Krautzeka 83/A
51000 Rijeka, Croatia
Phone: +385 (51) 770 447
Fax: +385 (51) 686 166
www.intechopen.com

InTech China

Unit 405, Office Block, Hotel Equatorial Shanghai
No.65, Yan An Road (West), Shanghai, 200040, China
中国上海市延安西路65号上海国际贵都大饭店办公楼405单元
Phone: +86-21-62489820
Fax: +86-21-62489821

© 2012 The Author(s). Licensee IntechOpen. This is an open access article distributed under the terms of the [Creative Commons Attribution 3.0 License](#), which permits unrestricted use, distribution, and reproduction in any medium, provided the original work is properly cited.

IntechOpen

IntechOpen